



TAMPEREEN TEKNILLINEN YLIOPISTO
TAMPERE UNIVERSITY OF TECHNOLOGY

MALIHEH SOLEIMANI

**FEASIBILITY STUDY OF MULTIAN TENNA TRANSMITTER
BASEBAND PROCESSING ON CUSTOMIZED PROCESSOR
CORE IN WIRELESS LOCAL AREA DEVICES**

Master's thesis

Examiner: Professors Mikko
Valkama and Jarmo Takala
Examiner and topic approved
by the Faculty Council of the
Faculty of Computing and
Electrical Engineering on 8
November 2013.

ABSTRACT

TAMPERE UNIVERSITY OF TECHNOLOGY

Degree Programme in Electrical Engineering

SOLEIMANI, MALIHEH: Feasibility Study of Multiantenna Transmitter Baseband Processing on Customized Processor Core in Wireless Local Area Devices

Master of Science Thesis, 62 pages, 1 Appendix page

January 2013

Major subject: Wireless Communication Circuits and Systems

Examiner: Professors Mikko Valkama and Jarmo Takala

Keywords: Wireless Local Area Network, Baseband Processing, Parallel Processing, Physical Layer, Software Defined Radio, Vector Processor.

The world of wireless communications is governed by a wide variety of the standards, each tailored to its specific applications and targets. The IEEE802.11 family is one of those standards which is specifically created and maintained by IEEE committee to implement the Wireless Local Area Network (WLAN) communication. By notably rapid growth of devices which exploit the WLAN technology and increasing demand for rich multimedia functionalities and broad Internet access, the WLAN technology should be necessarily enhanced to support the required specifications. In this regard, IEEE802.11ac, the latest amendment of the WLAN technology, was released which is taking advantage of the previous draft versions while benefiting from certain changes especially to the PHY layer to satisfy the promised requirements.

This thesis evaluates the feasibility of software-based implementation for the MIMO transmitter baseband processing conforming to the IEEE802.11ac standard on a DSP core with vector extensions. The transmitter is implemented in four different transmission scenarios which include 2x2 and 4x4 MIMO configurations, yielding beyond 1Gbps transmit bit rate. The implementation is done for the frequency-domain processing and real-time operation has been achieved when running at a clock frequency of 500MHz.

The developed software solution is evaluated by profiling and analysing the implementation using the tools provided by the vendor. We have presented the results with regards to number of clock cycles, power and energy consumption, and memory usage. The performance analysis shows that the SDR based implementation provides improved flexibility and reduced design effort compared to conventional approaches while maintaining power consumption close to fixed-function hardware solutions.

Preface

The research leading to this Master of Science Thesis was carried out within the Parallel Acceleration (ParallaX) project, funded by the Finnish Funding Agency for Technology and Innovation (Tekes). The work was also supported by Broadcom Corporation (earlier Renesas Mobile). The research work was carried out during the year 2013 at the Department of Electronics and Communications Engineering, Tampere University of Technology, Tampere, Finland.

I would like to thank my supervisor Prof. Mikko Valkama for the given opportunity and his enthusiastic support and guidance during this research. It was a great pleasure for me to work under his supervision and I had this opportunity to learn a lot from him. I would also like to thank Prof. Jarmo Takala for his valuable guidance and advices through this research. I would like to extend my gratitude to my friends, M.Sc. Lasse Lehtonen and M.Sc. Mona Aghababaeetafreshi for sharing their works and experiences on this research. I am also thankful to Juho Pirskanen, Hannu Talvitie and Ekaterina Pogossova from Broadcom Corporation for sharing their knowledge.

I would like to express my warmest thanks to my husband, Hossein Saghlatoon, for his patience, endless support and advices given through all the ups and downs of my studies.

I would like to extend my appreciation to my brother, Dr. Mohammad Reza Soleymaani for his constant support, guidance and advices during all years of my studies.

Finally, I would like to express my utmost gratitude and respect to my beloved family, especially my mother to whom I owe whatever I have achieved, for her unlimited love, invaluable support and encouragement in every possible way she could.

Tampere, December 2013

Maliheh Soleimani

TABLE OF CONTENTS

TERMS AND DEFINITIONS	vi
1. INTRODUCTION	1
1.1. Background and Motivation	1
1.2. Scope of the Thesis	3
1.3. Outline of the Thesis	3
2. IEEE802.11ac STANDARD	5
2.1. Overview of the IEEE802.11 Standards	5
2.2. IEEE802.11 Physical Layer Architecture	6
2.2.1. Physical Layer Convergence Protocol	6
2.2.2. Physical Medium Dependent	8
2.3. IEEE802.11 Medium Access Control Specifications	8
2.3.1. Carrier Sensing Mechanisms	8
2.3.2. Distributed Coordination Function	9
2.3.3. Point Coordination Function	9
2.4. An Overview of IEEE802.11a	10
2.5. High Throughput Specifications	10
2.5.1. High Throughput Physical Layer	10
2.5.2. High Throughput Medium Access Control	12
2.6. Overview of IEEE802.11ac Standard	12
2.7. Very High Throughput Physical Layer Specifications	13
2.7.1. Channelization	14
2.7.2. Modulation and Coding Scheme	15
2.7.3. MIMO Operation	16
2.8. Very High Throughput Medium Access Control Specifications	16
2.8.1. Frame Aggregation	16
2.8.2. Block Acknowledgement	17
2.8.3. Power Saving Enhancement	17
3. PROGRAMMABLE SOFTWARE DEFINED RADIO	18
3.1. Introduction	18
3.2. Real-Time Requirement	19
3.3. Very Long Instruction Word	20
3.4. Vector Processing	21
3.4.1. Vector Processing Units	21
3.4.2. Pros and Cons	21
3.4.3. Main Operations	23
3.4.4. Optimization Schemes	23
3.4.5. Power Consumption	24
3.5. Single Instruction Multiple Data	24
3.6. Vector Processors Deployment in Baseband Processing Wireless Modems ..	25

3.7. ConnX BBE32 DSP Core	26
4. IEEE802.11ac TRANSMITTER IMPLEMENTATION	29
4.1. Data Structure.....	29
4.1.1. Legacy Preamble	30
4.1.2. Very High Throughput Preamble	31
4.1.3. VHT Data Field	32
4.1.3.1. Stream Parser.....	32
4.1.3.2. Constellation Mapper.....	33
4.1.3.3. Low-Density Parity Check Tone Mapper	33
4.1.3.4. Space Time Block Coding	34
4.1.3.5. Pilot Insertion	35
4.1.3.6. Cyclic Shift Diversity	35
4.1.3.7. Spatial Mapping	36
4.1.3.8. Phase Rotation.....	36
4.2. Transmission Scenarios	36
4.2.1. Case a: 2x2 SU-MIMO Transmission.....	36
4.2.2. Case b: 4x4 SU-MIMO Transmission	38
4.2.3. Case c: 2x2 Antenna Configuration with 1x1 SU-SISO Transmission	39
4.2.4. Case d: 4x4 Antenna Configuration with 2x2 SU-SISO Transmission	40
4.3. Time and Frequency Parameters	41
5. RESULTS AND ANALYSIS.....	42
5.1. Software Implementation.....	42
5.2. Clock Cycles	42
5.3. Power Consumption	44
5.4. Energy per Bit	48
5.5. Memory Usage	50
5.6. Analysis	51
5.7. Related Works.....	52
6. CONCLUSION.....	54
REFERENCES	56
APPENDIX 1: CLOCK CYCLE RESULTS	61

TERMS AND DEFINITIONS

ACK	Acknowledgement
ALU	Arithmetic Logic Units
AP	Access Point
ASIC	Application Specific Integrated Circuit
BCC	Binary Convolutional Coding
BPSK	Binary Phase Shift Keying
CSD	Cyclic Shift Diversity
CSMA/CA	Carrier Sense Multiple Access/Collision Avoidance
CSMA/CD	Carrier Sense Multiple Access/Collision Detection
CTS	Clear-To-Send
DCF	Distributed Coordination Function
DL	Downlink
DSP	Digital Signal Processor
FFT	Fast Fourier Transform
FPGA	Field Programmable Gate Array
GI	Guard Interval
GPP	General Purpose Processor
GSM	Global System for Mobile Communications
HT	High Throughput
IEEE	Institute of Electrical and Electronics Engineers
LDPC	Low Density Parity Check
MAC	Medium Access Control
MCS	Modulation and Coding Scheme
MIMO	Multiple-Input Multiple-Output
MPDU	MAC Protocol Data Unit
MU	Multiple User
OFDM	Orthogonal Frequency Division Multiplexing
OSI	Open Systems Interconnection
PCF	Point Coordination Function
PHY	Physical Layer
PLCP	Physical Layer Convergence Protocol
PMD	Physical Medium Dependent
QAM	Quadrature Amplitude Modulation
RTS	Request-To-Send
SAP	Service Access Point
SDR	Software Defined Radio
SIMD	Single Instruction Multiple Data
STA	Station
SNR	Signal to Noise Ratio
STBC	Space Time Block Coding

VHT	Very High Throughput
VLIW	Very Long Instruction Word
VLSI	Very Large Scale Integration
Wi-Fi	Any WLAN products which is based on IEEE802.11 standard
WLAN	Wireless Local Area Networks

1. INTRODUCTION

In this chapter, the history of the wireless communications and Wireless Local Area Networks will be reviewed. Furthermore, the motivation and scope of the thesis will be described. In the final part, the rest of thesis will be outlined.

1.1. Background and Motivation

Wireless communications has always been a part of people's lives throughout the ages. Starting from simple speech to fire and smoke, humankind has been always trying to invent different ways to communicate over long distances. In the beginning of 19th century, with the help of science, more sophisticated communication methods were developed e.g. telegraph.

In the end of 19th century, the wired communications era was revolutionized by inventing telephone. Although, wired communications systems provide reliable, high information transmission rate over long distances, it always suffers from the limitation by wires. That limitation makes the idea of wireless communications more attractive. At first, because of the costs and complexity of electronics devices, the wireless/radio communication was mainly used in the military and broadcasting applications. Then, in the beginning of the 1990s, the first digital cellular networks working on Global System for Mobile Communications (GSM) were built. After that, the extremely increasing rate of mobile devices led to widespread use of mobile in the developed and developing countries.

However, wireless communication is one of the most vibrant areas in the communications field. Since the 1960's when the wireless communications became as an area of research interest and wired communications found limited, it has been exposed by a surge of improvements, research activities, and novelties. During the recent years, this field has been considerably developed due to several factors. First of all, explosive growth in the number of users whose demand for seamless service/connection has changed the wireless communication and even introduced new objectives. Besides, the intense progressive trend of the VLSI technology has allowed more complex systems to be integrated on a silicon chip. Meanwhile, the sophisticated signal processing methods have been supported by the fairly developed VLSI architectures to implement the novel algorithms in low power and low cost techniques [1, 2].

As the wireless communications systems have been increasingly involved into the many aspects of our daily lives, they have experienced much faster improvement rather than the rest of communications science. Furthermore, in the recent years, the word PORTABLE has introduced new features into the communication fields and devices.

Obviously, the conventional wired communication networks were not able to provide the connection along the mobility; therefore, the Wireless Local Area Network (WLAN)/Wi-Fi protocol was invented which was the sole practical solution to wireless connectivity in indoor environments.

For the first time, in 1997, the Institute of Electrical and Electronics Engineering (IEEE) introduced a new family of the communication standards titled IEEE802.11 for the WLAN systems. Due to the rapid growth and popularity of the wireless handheld devices, the wireless communication standards have been extremely developed during the past decade. However, more reliable, low power, low cost connections are also seen as crucial aspects to be supported by the WLAN standards.

Until now, the WLAN standard has substantially changed as new theory and implementation methods evolved; therefore several amendments have been released to correct or extend the previous versions such as IEEE802.11a and 802.11b. Essentially, the IEEE802.11 standards are described based on Physical (PHY) and Medium Access Control (MAC) layers. The MAC layer provides the functionalities to allow reliable data transmission, whereas the PHY features are used to govern the transmission and reception procedure [3].

Nowadays, a widespread application of the WLAN devices in the everyday life is witnessed; moreover, the increasing demand for higher speed connection and data throughput results in the new version of the IEEE802.11 called 802.11ac whose PHY and MAC features enhanced the throughput up to 6Gbps. It is worth mentioning that the most part of this improvement is made by the PHY features which are also the main focus of this study [4].

The IEEE802.11ac amendment actually overcame the limitations in the previous standards. The employment of wider bandwidth, Multiple-Input Multiple-Output (MIMO) transmission, higher number of spatial streams, and greater modulation size all together delivered the next leap in the performance of the Wi-Fi technology.

Another side of the wireless communications world is user equipment, such as mobile devices and modems which are also evolving, in their turn, in different features and functionalities. A clear majority of the current wireless devices are based on the implementation of the baseband digital signal processing algorithms in the Application Specific Integrated Circuits (ASIC) [5]. Although ASIC circuits allow sufficiently fast processing, they are fixed function which means they are not reconfigurable. On the other hand, as the number of communication standards and implementation algorithms continue to grow, the hardware implementations techniques moderately suffer from the lack of adaptability and compatibility to the new technologies. Particularly, the conventional modem designs are implemented in the silicon/semiconductor technology. With a new release, the previous designs are not mostly worth to be redesigned to accommodate the new specifications, as they would need expensive and time consuming procedures. Therefore a revolutionary method called Software Defined radio (SDR) technology introduced whose components that have been typically implemented in hardware are instead implemented using embedded devices or DSP cores. In fact, SDR aims to address

the fixed-function implementation difficulties by exchanging the fixed hardware implementation with a fully programmable platform [6, 7]. This programmable/configurable platform could be General Purpose Processor (GPP), Field Programmable Gate Array (FPGA), Digital Signal Processor (DSP), or any combination of them.

Software Defined Radio PHY layer wireless modems can be considered as the new trend in the field of wireless communications. In contrast with the dedicated hardware, the software based implementation can be easily modified to implement a wide variety of standards on the same platform. The usage of the software based solution results in flexibility, ease of design, time-to-market, and cost savings due to use of a single platform. However, the main concern is obtaining sufficient performance which can be achieved by having parallelism in the configurable platforms. The next issue is the energy efficiency in the fixed-function solutions which is not vincible by programmable SDR, thus the main aim is to improve the energy efficiency of the SDR solutions as close as the fixed-function methods. Although SDR solution would not reach the ideal case, if the gap is rational, then the cost savings in design will make the SDR solution desirable. Basically, making vector parallelism explicit in the programming is the key requirements of the SDR solution [8].

1.2. Scope of the Thesis

In this thesis, the feasibility of software based implementation using Very Long Instruction Word (VLIW) processor for the real-time operation of IEEE802.11ac transmitter full PHY layer baseband processing in four different transmission scenarios which include 2x2 and 4x4 MIMO configurations is addressed. As the processing platform, stemming from the requirements for very fast processing of huge amounts of data with transmission bit rates in the order of 1Gbps, the customized VLIW processor with vector processing capabilities is used. Such a software based implementation, if found feasible, can offer highly improved flexibility, much faster time-to-market, and highly improved possibilities to bringing in new transmission features and enhancements. In this project, the software development has been collaborative effort which leads to such an implementation capable of providing a huge part of the IEEE802.11ac requirements.

In the existing literature, a clear majority of the WLAN device implementations are fixed-function hardware based solutions [9]. In recent reports, some contributions have also been made towards the software defined radio concept [11]. However, in some works [11]-[14], only selected parts of PHY or MAC layer are typically targeted while other processing still relies on dedicated hardware.

1.3. Outline of the Thesis

The rest of thesis is organized as follows:

Chapter 2 presents the basics of the IEEE802.11 standards including both PHY and MAC layers. In the proceeding chapter, the 802.11ac and 802.11n amendments are also described in details.

Moreover, in Chapter 3, an overview of the vector processor in the various aspects such as architecture, pros and cons are given. In addition, the employed processor and some of its main features are also described.

In Chapter 4, a detailed description of the selected transmission scenarios of IEEE802.11ac standard is given. Furthermore, the software development environment and some of the employed optimization approaches are introduced.

The implementation results and analysis of the transmitter in the terms of power and energy consumption, clock cycle and memory usage are then provided in Chapter 5. Finally, Chapter 6 appends some concluding remarks to the thesis. In addition, the future status of the project will be also stated.

2. IEEE802.11AC STANDARD

In this chapter, all the Wireless Local Area Network (WLAN) standards belonging to the IEEE802.11 family will be reviewed. The general Physical (PHY) and Medium Access Control (MAC) layers features of this family are also described. The main discussed standard is the latest released called IEEE802.11ac, which is also referred to as the Very High Throughput (VHT); all the features related to these standards are also presented.

2.1. Overview of the IEEE802.11 Standards

The history of the IEEE802.11 standard dates back to 1997, when IEEE released the first wireless networking standard, the IEEE802.11 WLAN standard [15]. As it can be realized from its name, it belongs to the popular group of the IEEE802.x standards, such as IEEE802.3 standard for Ethernet and IEEE802.15 for Wireless Personal Area networks (WPANs) [16]. In fact, it can be said that IEEE802.11 WLAN specification was written to extend the functionality provided by 802.3 Wired LAN standard [17]. The IEEE 802.11 standard determines a set of Physical layer and Medium Access Control specifications to implement the WLANs communication systems in different frequency bands [18, 19]. Basically, until 1997, the major constraint for spreading the WLAN technology was the low penetration of the devices working based on the wireless technology. Since the popularity of wireless devices such as laptops and cell phones has increasingly risen, the number of users who want to access the internet not only in their offices but also in the other locations like restaurants, airport and shopping centers has also risen up, significantly. As a result, the WLAN technology has to be updated to fulfill the increasing demand for WLAN connection.

The IEEE802.11 was the basic version of the WLANs communication systems; therefore different amendments were released to extend or correct the previous specifications. The first released version of the WLAN standard family was IEEE 802.11a, but the first broadly accepted version was IEEE 802.11b (July 1999) which used the 2.4GHz frequency with 20MHz bandwidth and provided up to 11Mbps data rate. Until 2003, the main wireless protocol was IEEE 802.11b, but in order to achieve higher data rate another version was presented and authorized named IEEE 802.11g. From the operation frequency, bandwidth and number of spatial streams point of views, the IEEE 802.11b and 802.11g standards were similar, but IEEE 802.11g was using a new modulation scheme, namely, Orthogonal Frequency Division Multiplexing (OFDM), which resulted in up to 54 Mbps data rate. It was also compatible to IEEE802.11b, which was a novel feature in that time.

Then in 2009, the IEEE committee introduced and rectified a new version of WLAN standard, called IEEE802.11n, which brought new concepts into the wireless communications world. For the first time, the MIMO concept was exploited, which provided up to 600Mbps. This standard supports the usage of up to four spatial streams or 4x4 MIMO transmission system within two different channel bandwidths, 20 and 40MHz [20]. It is worth mentioning that IEEE802.11n is the version which has brought new format of the PHY layer, called High Throughput (HT), which will be discussed in section 2.4.

As mentioned earlier, the IEEE802.11 standard is a set of PHY and MAC specifications to support the wireless network. The PHY selects the appropriate modulation scheme with respect to the channel conditions given and provides the bandwidth; however the MAC layer governs how the available bandwidth shall be shared among all the wireless stations (STAs) [21]. Although several versions have been released to develop the protocol, the original MAC remained intact. It means that all the technology improvement evolved with the help of new PHY features such as the modulation and coding schemes, MIMO transmission concept, wider channel bandwidth and so on.

2.2. IEEE802.11 Physical Layer Architecture

The IEEE802.11 Physical layer is basically an interface between the medium access and the MAC layer, as depicted in Figure 1. It also defines the radio wave modulation and signalling characteristics for data transmission. Fundamentally, the 802.11 PHY layer consists of two generic functions, Physical layer Convergence Protocol (PLCP) and Physical Medium Dependent (PMD). Both functions will be discussed in the following. In general, the physical layer can be divided into five categories, which define different transmission techniques [22, 23]:

- Frequency Hopping Spread Spectrum (FHSS)
- Direct Sequence Spread Spectrum (DSSS)
- Infrared light (IR)
- High Rate Direct Sequence (HR/DS)
- Orthogonal Frequency Division Multiplexing (OFDM)

Each PHY layer has specific PLCP and PMD to control the transmission and reception procedure [24].

2.2.1. Physical Layer Convergence Protocol

Physical Layer Convergence Protocol (PLCP) determines a suitable mapping method for IEEE802.11 MAC Protocol Data Units (MPDUs) into a framing format appropriate for sending and receiving user data and information management among two or more STAs using the associate PMD system. [18]

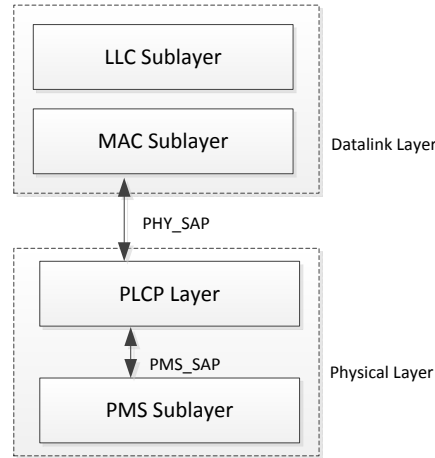


Figure 1. PHY and MAC sub-layers structure

Figure 1, illustrates how the data link and physical layers are connected to each other. According to Figure 1, the MAC sub-layer communicates with the PLCP through Physical Layer Service Access Point (PHY_SAP) by using a set of instructive commands or fundamental instructions. Basically, when the MAC layer commands the PLCP to operate, it prepares the MPDUs for the transmission. It is worth observing that the PLCP minimizes the MAC layer dependency on the PMD sub-layer by mapping the MPDUs into a suitable format for transmission. It also delivers the incoming frames from the wireless medium to the MAC layer.

The PLCP inserts preamble and header fields into each incoming MPDU from the MAC layer due to the following reasons:

- Preamble field is used to synchronize the transmitter and receiver. It is composed of two fields, synchronization and SFD (Start Frame Delimiter), depending on the utilized modulation and data rate, it may have different length.
- Header field, as shown in Figure 2, is placed after the preamble, which includes some transmission parameters. This field also comprises of four different fields. The first field is signal which has the required information regarding the transmitter data rate, which followed by service field reserved for the future use (set to zero). The third one is called length, which carries the information regarding the frame duration, and the last one is Cyclic redundancy Check (CRC) containing 16 bits which is used to detect bit error in the message with high reliability. Therefore, the receiver first verifies the CRC correction before any further processing.

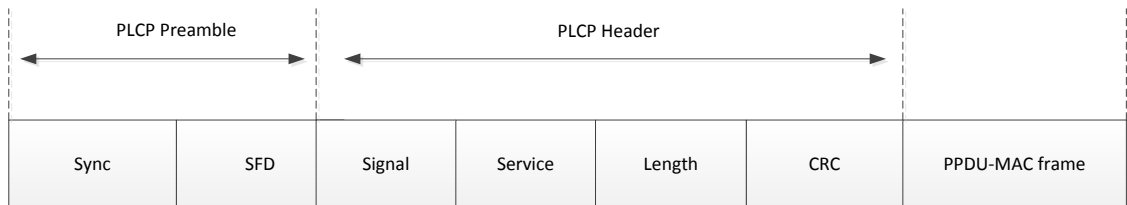


Figure 2. PLCP structure

In the end, the resulted frame (the MPDU and the additional preamble and header) is referred to as PLCP Protocol Data Unit (PPDU) [24].

2.2.2. Physical Medium Dependent

With reference to the provided definition for the PLCP, the Physical medium Dependent defines the data transmission and reception techniques between STAs and PHY entities through the wireless medium, including modulation and demodulation and hiving interference with air medium [25]. As it can be observed in Figure 1, PLCP and PMD communicate through the PMD_SAP to control the transmission and reception functions [24].

2.3. IEEE802.11 Medium Access Control Specifications

The Medium Access Control (MAC) layer is one of the sublayers of the data link layer in the Open Systems Interconnection (OSI) model. Principally, the MAC layer is a set of rules to determine how to access the medium and data link components, but the most important functionality of the MAC layer is addressing and channel access control that makes the communication of the multiple stations possible.

The key point is that the IEEE802.11 MAC layer is compatible with the Ethernet standard (IEEE802.3) at the link layer, that compatibility is resulted from the fact that these two standards are similar in terms of addressing and channel access [26]. It shall be also added that the Carrier Sense Multiple Access technique (CSMA) is also supported by IEEE802.11 MAC layer which makes the access to the shared wireless medium feasible [27]. According to CSMA technique, the STA is allowed to transmit when the channel is 'idle'; otherwise it has to postpone its transmission [28].

The MAC layer architecture supports two different fundamental access methods, the Distributed Coordination Function (DCF) and the Point Coordination Function (PCF). Besides these two key functions, the Hybrid Coordination Function (HCF), the Mesh Coordination Function (MCF), and their coexistence are included in the IEEE802.11 WLAN standard [29]. The simple distributed, contention based access protocol supported by CSMA/CA technique is the basic MAC protocol for IEEE802.11 [28].

2.3.1. Carrier Sensing Mechanisms

Except the time when the STA is transmitting and therefore knowing that the medium is busy, it requires an additional mechanism to check the state of channel. Carrier Sensing methods are used (by STAs) to determine whether the medium is busy or not. In the standard, two main carrier sensing mechanisms are defined, namely, Physical Carrier Sensing (PCS), which is supported by PHY layers, and Virtual Carrier Sensing (VCS) [30]. However, a third carrier sensing method is also used called Network Allocation

Vector (NAV) provided by MAC specifications. The state of medium will be determined by using either PCS or VCS [31].

The PCS technique must be provided by the PHY layers. In fact, the PCS is an obligatory carrier sensing method in any PHY layer to state the medium status; the responsible function for this purpose is called Clear Channel Assessment (CCA). In this method, the channel state can be determined by using the PLCP layer, if it indicates that the channel is 'Idle', the transmission procedure can be initiated. The busy indication should be raised when another signal is detected in the medium; in this case, the station would enter a contention window and the transmission is delayed until the end of the impending transmission.

The VCS technique ascertains the state of medium by spreading the reservation information announcing the usage of medium. For instance, the transmission and reception of the Request-To-Send (RTS) and Clear-To-Send (CTS) frames (which happens before the actual data transmission) is an example of distributing the reservation information to the medium [32]. When a node has a packet to transmit, it first ensures that no other node is transmitting by sending the RTS frame. When the receiving station is ready to receive the data, it responds by sending a CTS frame. Once the RTS/CTS exchange is complete, the transmitter node can transmit its data frame without any concern regarding the interference or any other problem. The medium is definitely idle and reserved during a certain period of time which is defined by RTS and CTS frames, in fact this period is enough to transmit the actual data frame and return the Acknowledgement frame (ACK). The medium reservation can be done by station which either receives the RTS or the CTS frames. [18]

2.3.2. Distributed Coordination Function

The DCF is the fundamental access method in the IEEE802.11 MAC layer which is used to support asynchronous data transfer on a best effort basis [33]. DCF provides distributed, but coordinated access in such a way that only one station can transmit [26]. In fact, in the case that the medium is not sensed to be busy, the transmission may proceed; otherwise it may be deferred. Therefore, the presence of the DCF is mandatory in all types of station [34]. It is also known as Carrier Sense Multiple Access with Collision Avoidance (CSMA/CA). The Carrier Sense Multiple Access with Collision Detection (CSMA/CD) has not been used due to the fact that STA is not capable to listen to the channel while transmitting.

2.3.3. Point Coordination Function

The PCF access method is an optional technique which is only applicable in the infrastructure network configurations. In this method, one Point Coordinator (PC) is required to determine which station will transmit. Basically, this operation is done based on the polling mechanism and the PC is playing the role of the polling master. It can be said

that the PCF is a contention free service provider, which has some special service points to assure the provided medium is without contention [18, 35].

2.4. An Overview of IEEE802.11a

The latest two popular versions of the WLAN standards, including IEEE802.11n and IEEE802.11ac, entail the fundamental PHY and MAC specifications of the IEEE802.11a. Consequently, the key and common specifications of the 802.11a will be discussed.

In 1999, the IEEE released the first established WLAN standard, IEEE802.11a which was designed to operate in the 5GHz frequency range within a 20MHz channel bandwidth divided into 64 subbands. The 802.11a is a packet based radio interface and uses an OFDM based encoding scheme rather than FHSS or DSSS to send the data. Accordingly, the assigned bandwidth is channelized in such a way that 48 subcarriers out of 64 are used for data transmission, 4 subcarriers are used as pilot, and the rest are null. The subcarriers design was based on FFT size of 64, as shown in Figure 3. Based on the allocated PHY specifications, the IEEE802.11a standard was expected to support up to 54Mbps for business and office applications, but it was suffering from the limited coverage range, delayed time-to-market and high cost.

The 802.11a MAC unit works based on the Carrier Sense Multiple Access, Collision Avoidance (CSMA/CA) in which the transmitter listens to figure out the status of the medium either busy or idle. In the medium is idle, the transmitter sends a short Request-To-Send (RTS) package containing the information regarding the package. Then, the transmitter waits for the response from the receiver before starting the transmission. Meanwhile, other transmitters within the reach area also receive the RTS package which helps them to estimate how long the transmission will take.

2.5. High Throughput Specifications

The IEEE802.11n standard is the High Throughput amendment to the 802.11 standard. The key features of the 802.11n are the application of MIMO and OFDM concepts which lead to significant increase in the data rate in 40MHz channel bandwidth. With the aid of these two techniques, the data rate of 600Mbps was obtained. [20]

Regarding the High Throughput IEEE802.11 standard, two groups of specifications will be discussed. The first one is the PHY specifications, and the second is MAC.

2.5.1. High Throughput Physical Layer

The HT PHY is based on the Orthogonal Frequency Division Multiplexing (OFDM) which is well suited for the wideband systems in the frequency selective environment. In addition, OFDM is bandwidth efficient as multiple data symbols can be transmitted on different orthogonal frequencies or subcarriers, simultaneously. Therefore, the OFDM provides better spectral efficiency and immunity to multipath fading. [36]

In the HT PHY, in order to modulate the data subcarriers, Binary Phase Shift Keying (BPSK), Quadrature Phase Shift Keying (QPSK), 16-Quadrature Amplitude Modulation (16-QAM) and 64-Quadrature Amplitude Modulation (64-QAM) are used as the modulation scheme. The Forward Error Correction (FEC) or the convolutional coding technique is deployed with the coding rate of $1/2$, $2/3$, $3/4$, or $5/6$. As an optional feature, the Low-Density Parity-Check (LDPC) coding method can be also used. These features are known as Modulation and Coding Scheme (MCS) to define the modulation size and coding rate. The notable point regarding the MCS definition in the 802.11n is that it also determines the number of spatial streams. It means that MCS parameters include modulation, coding rate and spatial stream number which bring complexity in MCS set selection. [28]

The available channel bandwidths in the IEEE802.11n standard are 20MHz and 40MHz. The 20MHz channelization is based on the using the FFT size of 64 including 64 subcarriers to send the data. Of these, 4 pilot subcarriers are inserted at the positions $\{-21, -7, 7, 21\}$, the 56 data subcarriers are located at $\{-28, \dots, -1, 1, \dots, 28\}$. The rests are null which are at positions $\{-32, -29, 0, 29, \dots, 31\}$. Figure 3 depicts the channelization in the case of 20MHz channel bandwidth. [28]

The 40MHz subcarrier design is based on using FFT size of 128 so that 128 subcarriers are available to carry the data. There are totally 14 null subcarriers located at $\{-64, \dots, -59, -1, 0, 1, 59, \dots, 63\}$, and there are 114 populated subcarriers at the rest of positions. Of these, 6 subcarriers are pilot in the positions $\{-53, -25, -11, 11, 25, 53\}$; the 108 remaining subcarriers are dedicated to the data placed at $\{-58, \dots, -2, 2, \dots, 58\}$ except the pilot ones. Figure 4 shows the channelization for 40MHz bandwidth. [28]

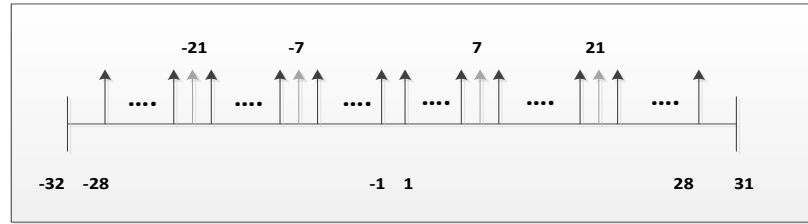


Figure 3. 20MHz channelization

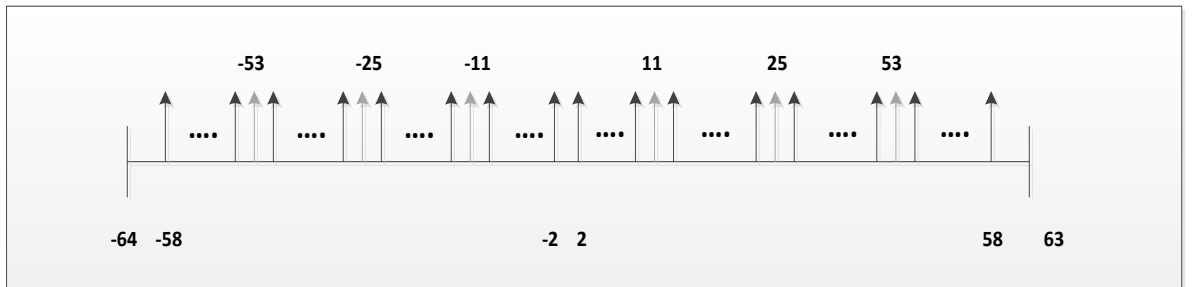


Figure 4. 40MHz channelization

It is worth pointing out that there are some other optional features such as Space Time Block Coding (STBC) scheme, 400ns Guard interval (GI) and beam forming which are applicable at both transmission and reception sides. With the help of these PHY features, a maximum data rate of 600Mbps is available in the 802.11n standard.

The HT PHY includes two main functional entities, namely, the PLCP and PMD functions which are similar to the basic model for the 802.11 standard, explained in section 2.2.

2.5.2. High Throughput Medium Access Control

Although, it was found that without any enhancement in the MAC layer, the end user would benefit from the PHY layer improvement. Therefore, the HT MAC layer is almost same as the original one, but still some enhancement has been made to improve the efficiency in the form of frame aggregation and block acknowledgement [31]. Since, the MAC mechanisms used in the 802.11n are similar to the 802.11ac; these changes will be discussed in the VHT part, comprehensively.

2.6. Overview of IEEE802.11ac Standard

As the IEEE802.11n amendment became popular and matured enough in the market, in May 2007 the IEEE committee organized a new study group to investigate the feasibility of Very High Throughput (VHT) technology. This group released the first draft version in 2011 which was capable of providing data rate up to 6.93Gbps, under certain circumstances. This considerable high data rate is coming from standardized modification to both PHY and MAC layers of the IEEE802.11n standard which will be described in the following sections.

The key requirement of the IEEE802.11ac is the compatibility with the previous amendments, IEEE802.11a and IEEE802.11n in the frequency band of 5GHz. It must be noted that the IEEE802.11ac was restricted to the frequency band lower than 6GHz, as the higher frequency band was dedicated to the next generation of WLAN standard, called IEEE802.11ad. Although in the 802.11ac standards, both PHY and MAC layers specification have been changed, the major part of the data rate enhancement is stemming from the new PHY features.

The first generation of the IEEE802.11ac devices must provide at least the previous PHY requirements of the 802.11n such as up to three spatial streams; moreover they are also expected to include the 256-QAM modulation. The rest of PHY features like STBC and LDPC are expected to be employed in the next generations of the 802.11ac devices. However, the usage of the optional properties results in both throughput and robustness enhancement of the wireless systems. Figure 5 presents all the mandatory and optional PHY features for the IEEE802.11ac. The principal transmitter and receiver block diagram in the IEEE802.11ac are also presented in Figure 6 and Figure 7, respectively. However, main focus of this thesis is on the transmitter chain.

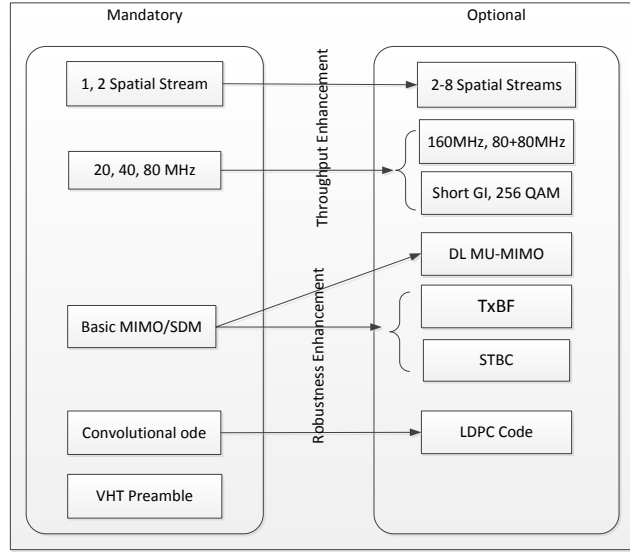


Figure 5. PHY layer features for IEEE802.11ac

2.7. Very High Throughput Physical Layer Specifications

The main PHY features and enhancements for the IEEE802.11ac standards to increase the data rate include the wider channel bandwidth, efficient modulation and coding schemes, higher number of spatial streams and downlink multiuser MIMO (DL MU-MIMO) transmission.

In the previous amendments, the channel bandwidths of 20MHz and 40 MHz were used. However, the bandwidth in the 802.11ac was expanded to 80MHz and 160MHz which improve the data rate, significantly. The capability of using non-contiguous channels to make wider channel bandwidth and better fit into the available spectrum is one of the main remarkable features of IEEE802.11ac PHY layers. By this means, two non-contiguous 80MHz channels can define a 160MHz channel (80+80 MHz). The IEEE802.11ac standard also exploits the newly defined 256 Quadrature Amplitude Modulation (QAM) with the different coding rates which considerably increase the data rate.

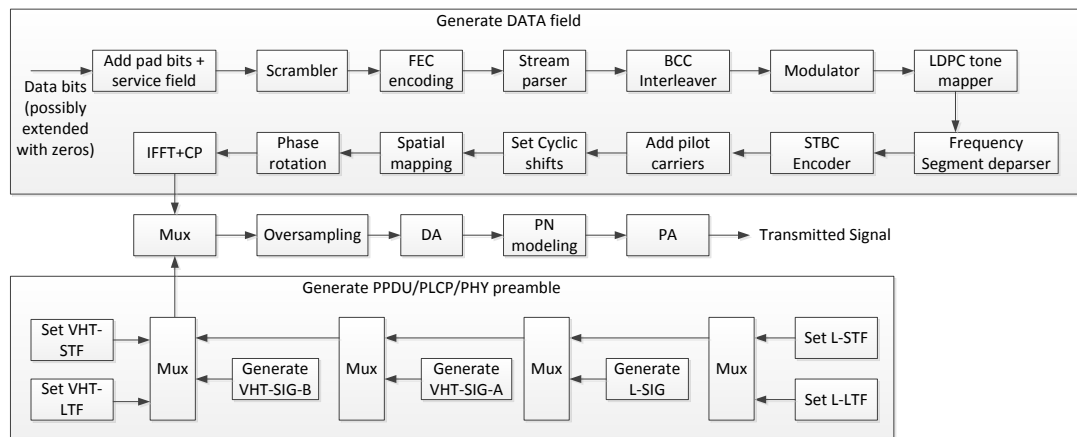


Figure 6. Functional transmitter chain

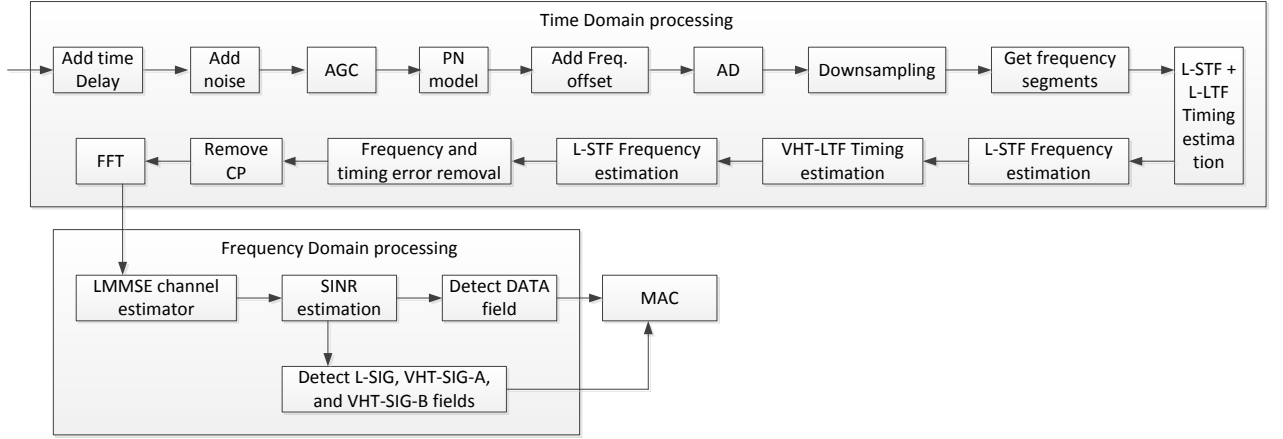


Figure 7. Functional receiver chain

In addition to the channel bandwidth and modulation and coding scheme improvement, the DL MU-MIMO feature is defined in the 802.11ac that allows an Access Point (AP) to transmit data streams to the multiple users, simultaneously. This feature can be also discussed in both terms of MAC and PHY layers.

2.7.1. Channelization

The 20MHz and 40MHz channelization for the 802.11ac is similar to the 802.11n standard, therefore, we only define the design for 80MHz and 160MHz channels. The 80MHz subcarrier design is based on the 256 FFT points meaning that 256 subcarriers are available to carry the data. The subcarriers indices start from -128 to 127, as depicted in Figure 8. There are 14 null subcarriers which are located at $\{-128, \dots, -123, -1, 0, 1, 123, \dots, 127\}$, and 8 pilot subcarriers which are at positions $\{-103, -75, -39, -11, 11, 39, 75, 103\}$. The rest of subcarriers (234 subcarriers) are data subcarriers placed at $\{-122, \dots, -2, 2, 122\}$ except those 8 indices which are occupied by the pilot subcarriers. [28]

In the case of 160MHz channel, the FFT size is 512 including 28 null subcarriers, 16 pilot subcarriers, and 468 data subcarriers. The 160MHz subcarrier structure is made of two 80MHz portions, in such a way that the lower and upper 80MHz populated subcarriers are mapped to -250 to -6 and 6 to 250, respectively. The null subcarriers are located at $\{-256, \dots, -250, -129, \dots, -127, -5, \dots, 5, 127, \dots, 129, 251, \dots, 255\}$, the 16 pilots are at $\{\pm 231, \pm 203, \pm 167, \pm 139, \pm 117, \pm 89, \pm 53, \pm 25\}$. The remaining subcarriers are the data subcarriers. Figure 9 shows the 160MHz channelization [28]. The new channel bandwidth definition brings more flexibility in the term of channel assignment to avoid any overlap to other channels or even radars.

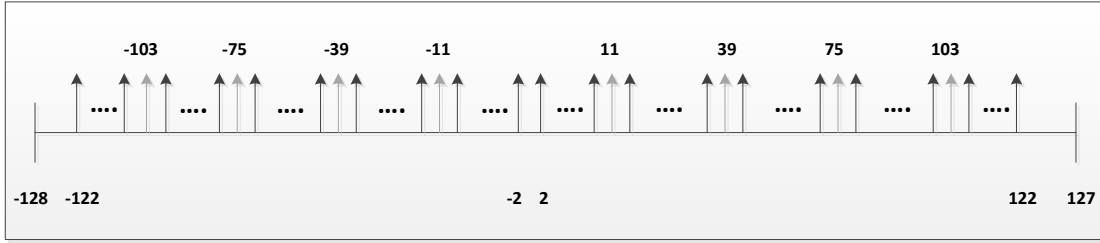


Figure 8. 80MHz channelization



Figure 9. 160MHz channelization

2.7.2. Modulation and Coding Scheme

In the IEEE802.11ac, the modulation schemes include Binary Phase Shift Keying (BPSK), Quadrature Phase Shift keying (QPSK), 16/64/256 Quadrature Amplitude Modulation (QAM) to modulate the OFDM subcarriers. In addition, Binary Convolutional and Low Density Parity Check coding methods with the variety of coding rates of $1/2$, $2/3$, $3/4$ and $5/6$ are applicable. These coding methods (with different coding rate) in combination with the available modulation schemes, referred as Modulation and Coding Scheme (MCS) in the 802.11ac, are the new PHY features to enhance the throughput. Compared to the IEEE802.11n, the MCS set selection in the 802.11ac is much simpler as it only offers 10 MCS sets, as shown in Table 1. [28]

The usage of 256-QAM has the potential to improve the transmission rate because of the fact that 8 bits can be sent on each subcarrier, basically it bring 33% increase in the data rate. However, by using the 256-QAM modulation scheme, the system sensitivity to the noise and synchronization also increases which emphasis on the importance of using error correcting methods to robust the system [37]. For instance, IEEE802.11ac includes the LDPC coding to achieve better performance. Consequently, the modulation size increase would improve the data rate if the link quality permits which means the link quality shall be remain acceptable by increasing the modulation size [28].

For instance, 600Mbps is the maximum achievable data rate in 802.11n using four spatial streams and 40MHz channel bandwidth. However, for the same configuration and using 256-QAM modulation, IEEE802.11ac obtains 800Mbps data rate.

Guard Interval (GI) is also used to combat the effect of frequency selectivity and multipath effect which is similar to the 802.11n standard.

2.7.3. MIMO Operation

In IEEE802.11ac, after increasing the channel bandwidth, one of the major techniques used by IEEE802.11ac to increase the throughput is the extension of the spatial streams from 4 to 8. Therefore, for the first time, an IEEE802.11ac AP shall be built in such a way to support 8 spatial streams which require an antenna array with 8 independent radio chains and antennas. The deployment of antenna array also brings the beam forming capability to steer the antenna beam toward a specific receiver.

One of the IEEE802.11ac target design was the multiple transmission for the multiple users (MU-MIMO). By this means, instead of having single transmitter and receiver in the same area, the MU-MIMO provides the concept of spatial sharing of channel where the same channel can be used in the different areas by the same access point. Furthermore, the MU-MIMO is advantageous for the AP to have more antennas than total number of spatial streams to have diversity gain and cleaner beam. By this means, the network capacity is also increasing. [38]

Table 1. MCS values for IEEE802.11ac

MCS Index Value	Modulation	Code Rate
0	BPSK	$\frac{1}{2}$
1	QPSK	$\frac{1}{2}$
2	QPSK	$\frac{3}{4}$
3	16-QAM	$\frac{1}{2}$
4	16-QAM	$\frac{3}{4}$
5	64-QAM	$\frac{2}{3}$
6	64-QAM	$\frac{3}{4}$
7	64-QAM	$\frac{5}{6}$
8	256-QAM	$\frac{3}{4}$
9	256-QAM	$\frac{5}{6}$

2.8. Very High Throughput Medium Access Control Specifications

Although the major changes to increase the throughput are applied into the PHY layer, there are few MAC changes in different terms in the IEEE802.11ac to make the PHY faster.

2.8.1. Frame Aggregation

As mentioned previously, if the medium is sensed as busy the AP has to postpone its transmission, it results in contention and collision in the medium. For the first time,

IEEE802.11n introduced a frame aggregation mechanism to reduce the collision and contention, and also overcome the theoretical throughput limit to achieve VHT targets [33]. According to this method, a station with a number of frames to transmit can combine/merge them into one aggregate MAC frame. By this combination, the fewer frames are sent so that the contention time is reduced [39].

2.8.2. Block Acknowledgement

In the previous standards, the receivers were transmitting the ACK packet to the transmitter to make it sure the data frame is received properly. But in the IEEE802.11ac, the new MAC feature allows the receiver to send a single ACK package to cover a range of received data frames.

This method is applicable in the case of video transmission or the high data rate transmission. It should be noted that if one frame is lost or corrupted, a long delay will be needed to do the re-transmission. This delay is only problematic in the real-time transmission; otherwise it is not often a problem. [39]

2.8.3. Power Saving Enhancement

Due to the fact that most of the WLAN based devices are still battery-powered, and meanwhile there are several other units in those devices which use the battery power, the power saving methods are worth to study. In IEEE802.11ac several power saving techniques has been introduced and addressed which are described as follows.

One of the power saving features in the 802.11ac is the presence of higher rate. In other words, the power consumption is dependent on the data rate. The higher the data rate, the shorter the transmission burst which means the reception burst is also shorter. By this means, the power consumption at the receiver side would also decrease, but it is not significant. [39]

A new feature is also introduced in the IEEE802.11ac, which permits the client to switch off its radio circuits when the AP indicates that a transmission is impending for another client. Besides all these features, the capability of the beam forming to an arbitrary direction increases the signal-to-noise ratio (SNR), which results in longer battery life. [39]

3. PROGRAMMABLE SOFTWARE DEFINED RADIO

In this chapter, the history of vector processors will be reviewed; moreover, one of the most important requirements for the software or hardware systems called real-time operation will be studied. Then, to achieve high performance and power efficiency, three different processor architectures will be studied. Furthermore, the programmable/configurable SDR platform and their deployment in the baseband processing wireless modem will be discussed. In the end, one specific application processor called ConnX BBE32 [40], which is used in the project, will be deliberated.

3.1. Introduction

Today, majority of the Central Processing Units (CPU) implement the architectures in such a way to execute instructions in the vector processing manner on the multiple data sets, they usually referred as the Single Instruction, Multiple Data (SIMD). On the other hand, there are some processors which are executing multiple instructions on the multiple data sets in a vector wise procedure, and so called Multiple Instruction, Multiple Data (MIMD). It is worth mentioning that the first category is more commonly used and designed for general computing purposes whereas the second one is usually dedicated to a particular application and designed for specific purposes. In the continuation, the history of the vector processors will be revealed.

By starting the Solomon project in the early 1960s at Westinghouse, the development of the vector processors started. The main target was considerably increasing the arithmetic performance by deploying several simple co-processors controlled by one main master CPU. In that architecture, applying one instruction to a long set of data (in the vector/array) was allowed [41]. This effort continued and finally the first commercial vector processor was delivered in 1972 which had only 64 Arithmetic Logical Units (ALUs). By the way, the first successful implementation of the vector processors belongs to the Control Data Corporation STAR-100 and the Texas instruments Advanced Scientific Computers (ASC) which had basically one ALU providing both scalar and vector computations. But in 1976, for the first time, the vector processor was successfully exploited in the famous design known as Cray-1. This trend followed till now that we witness different kinds of the vector processors e.g. Cray-XMP, Cray-YMP [41].

The vector processor is a processor which is capable to execute the operation on multiple operands. The operands to the instructions are complete vectors instead of the one element and their processing is done in a vector fashion. Furthermore, the vector pro-

processors are addressed as special purpose computers to match a set of scientific arithmetic operations which take long time to be processed, and are accessed with low locality, yielding poor performance from the memory hierarchy [42]. The main feature of the vector processor is to pipeline both data sets and instructions to obtain lower decoding time; the Figure 10 depicts the mentioned concept simply. [43]

Wireless communication is one of the most computationally based fields which is demanding for a huge amount of workloads, and also introduces numerous difficulties to the design and implementation process. In this field, all the requirements must be performed by a small mobile device and must be accomplished by a small battery which is responsible to power the system. The main aim of the wireless communication industry is to provide a seamless end-user service along high data rates, meanwhile the power is limited. To achieve high performance and power efficient solutions, three categories of the processors can be chosen. The first one is the application specific processors which are very expensive and fixed-function. The second category is the usage of multi-core processors which consist of several independent CPU lead to high power consumption. The last but not least is the parallelism processors which exploiting the parallelism concept to gain higher performance while keeping the power consumption affordable. From the platform point of view, the parallel processors can be categorized into three classes to compromise on both targets, namely, Very Long Instruction Word (VLIW), vector processing and SIMD which will be discussed in the following.

3.2. Real-Time Requirement

In the recent years, the real-time processing/computing/operation has emerged as an important discipline in the computer science and engineering. With the intensive growth of the computational power, more systems are being implemented in the software based solution to exploit the flexibility and sophistication afforded by the software implementation. However, as the real-time implementations are getting more complicated, the software design styles have been brought to a higher level.

Broadly speaking, real-time processing subjects the system to a real-time constraint which means the system has to response to the input within a specific time period. The real-time constraint is often referred to as operational deadline for each machine instruction. Thus, the ‘time’ is a source of fundamental concern in the real-time systems, and all the instruction must be scheduled and executed to meet their timeliness requirements. The timeliness requirements can be classified into hard real-time where failure to meet a deadline is treated as fatal system failure; and the soft real-time where an occasional missed deadline may be tolerated.

In the field of the Digital Signal Processing (DSP), a real-time system should process the input and output samples continuously in the time that it takes to input and output the same set of samples independent of the processing delay. That means the mean of the processing time per sample is not greater than the sampling period which is also the reciprocal of the sampling rate.

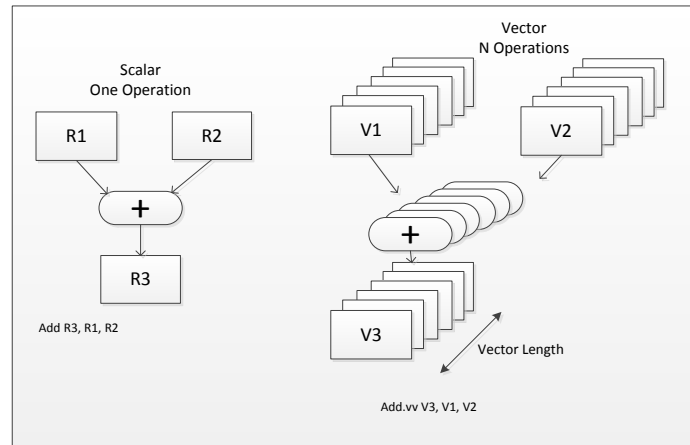


Figure 10. Principles of scalar and vector instructions

In the real-time systems, there are several challenging and complex issues to deal. The first one is the fact that the real-time systems are components of a larger system which collaborates with the physical world. The physical world treats in a non-deterministic manner, full of events occurring asynchronously, concurrently, and in an unpredictable order. In such a condition, the real-time systems must respond properly and in a timely manner. The second complexity is the concurrency of the physical world which subjects the real-time systems to synchronize a multiple concurrent instruction arising in the environment [49].

The main characteristics of the real-time systems are the reliability and availability as any failure or error may cause considerably cost [49].

In the processors, we are able to assess the real-time performance of the utilized core with the aid of the number of clock cycles. In fact, each processor has a specific operating frequency whose inverse value is equal to the time given to processor to execute instructions. Furthermore, the number of required clock cycles, profiled with appropriate tools, to execute a program shows the capability of the processor for real-time computing. For instance, a DSP core has an operating frequency of 100MHz, and needs 100 clock cycles to accomplish a program whose real-time constraint is 3 μ s. According to the processor frequency, the processing time of each clock cycle is equal to 10ns; therefore, the total time of program execution is 1 μ s which means the processor can fulfil the timeliness requirement.

3.3. Very Long Instruction Word

VLIW is a processing technique which dates back to 1980's. The term VLIW refers to the size of each instruction accomplished by the processor, this instruction is very long compared to the instruction word size utilized in the common processors.

VLIW can be outlined as a processor architecture which is taking advantage of the instruction parallel level. In other words, VLIW processor allows the program to specify multiple operations to be executed concurrently; such operations are actually packed into one large instruction. In this techniques, when one instruction has been fetched all the corresponding operations are issued in parallel. The VLIW lead to a very significant

improvement which is simple hardware in a way that number of functional units can be increased without need to any additional sophisticated hardware.

3.4. Vector Processing

Vector processing is a technique in which one instruction is executed on an entire vector. The operands to the instructions are complete vectors instead of one element. Fundamentally, in the vector processors, the basic idea is to read the sets of data elements into the vector registers, and then the operation is executed on those registers. At the end, the final results are dispersed back into the memory. In the vector processing technique, a deep level of pipelining is used to execute the element operations; meanwhile the clock frequency can be increased. Although, deep pipeline introduces complication from the control perspective, in the vector processing as the data elements are independent so that this problem is simply overcome.

3.4.1. Vector Processing Units

The following explained blocks are the most commonly used components in the vector processors.

The first block is Vector Register whose length determines the maximum vector length. These registers usually have both read and write ports. These vectors are actually specialized registers to perform the vector calculations so that they are faster and have low startup costs. The vector register helps in significantly higher performance compared to earlier models of the vector processors. [44]

The second one is vector functional units (FUs) which are completely pipelined and performing new instruction in every cycle. Arithmetic and logical operations are done within these units, moreover the load and store operation are also processed by the FUs.

The vector Load-Store Units (LSUs) are the third important blocks in the vector processors which are responsible to move the vectors between memory and registers.

The last but not least is the Scalar registers that contain single elements or integers to make link between LSUs, FUs and registers. In addition, they carry out the logical operations on the scalars.

It shall be noticed that one vector instruction indicates a huge amount of computation. This is as a matter of the fact that each instruction is done on the multiple data sets, at the same time. Figure 11 depicts the main blocks in a typical vector processor.

3.4.2. Pros and Cons

In order to answer the question, "Is the usage of vector processor beneficiary or not?", the negative and positive aspects of them shall be reviewed. Then, regarding the application, the significance of vector processor use will be clarified.

In the following, we first address the pros.

- The computation/execution of each operation in a single vector instruction has no

data dependency which gives the capability of a very deep pipeline execution without any data missing.

- Every single vector instruction implies lots of work which sounds like the operation of the whole loop and fewer instructions for execution. Consequently, the required instruction bandwidth is much smaller.
- The access pattern for each vector instruction is known, which makes fetching vector (with appropriate adjacent elements) from a set of heavily interleaved memory banks very well organized. Using this method, one memory access has been initiated to the entire vector rather than to the single word of the vector so that the latency of initiating to the main memory is considered only once for the entire vector instead of each vector word.
- As a matter of the fact that fewer instructions are needed, the smaller the size of program code. In addition, by execution one loop, many branches can be hidden in one instruction.

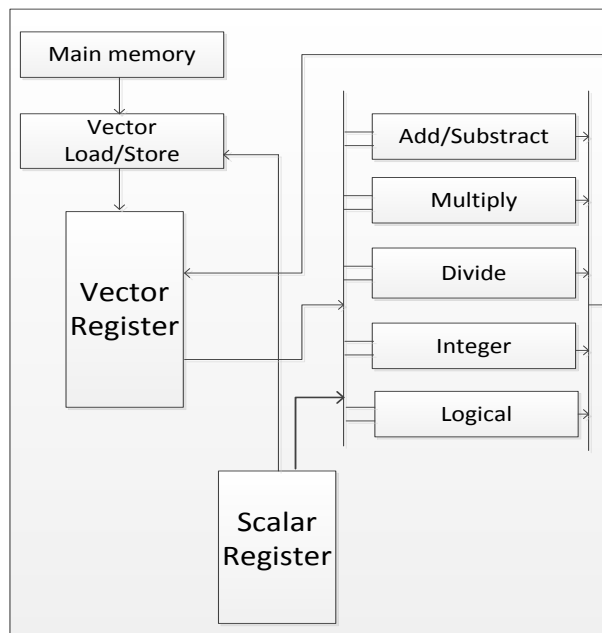


Figure 11. Vector processor structure

- Due to the operation circumstance during the vector processing, only Functional Unit (FU) and the register buses feeding need to be powered. Therefore, the rest of units such as fetch unit, decode unit, ROB and etc. can be powered off so that the power consumption will reduce.

Until here, the advantages of vector processor application became clear, now the disadvantages will be explained:

- Although the vector processors can be used widely, they work very well with those data executed in high parallel level.
- To work efficiently, it needs to be fed with large amount of data.

- On the scalar data processing, there is a deep lack of good performance which makes the vector processors inefficient compared to the normal processors.
- The cost of vector processors compared to the other processors is relatively high, which is resulting from the need of specific design for each application, high speed on-chip memories, difficulty in packaging and keeping the innovative architectural design to achieve lower cost.
- Due to the vectorized execution, there is high level of complexity in the codes. It has been also found that sometimes the code alignment shall be done manually to achieve better performance.

Besides all the aforementioned parameters, generally the performance of the vector processors is still dependent on the length of operand vector, data dependencies and structural hazards which will even introduce more difficulties.

All these positive and negative aspects altogether contribute in specific features to the vector processors and indicate that vector processors need necessary modifications to become widely popular. [43]

3.4.3. Main Operations

Although the vector processors are operating similar to the normal processors, due to their specific features and architecture, the main operational mechanism is worth studying.

A typical vector processor is capable to add two vectors to produce a third vector. It can also subtract two vectors to generate a third one. Multiplication and division of two vectors to make a third vector is applicable in the vector processors.

By having special Load and Store units, it is possible to read and write vectors from or to the memory similar to the normal processors, but in the vector processors these kinds of processes can be executed faster.

Under the certain circumstances depending on the processor, the following instructions can be also done. Inner product (multiplication and accumulation) and outer product of two vectors are feasible to be done, but the important point is that these operations produce an array from vectors whose elements can be used as primitive data, yet. Product between arrays can be done only for small arrays.

3.4.4. Optimization Schemes

From the optimization point of view, different techniques have been used and applied into the vector processors to achieve the most efficient performance in terms of power, code size and speed.

First of all, the usage of banked-memory reduces the latency for load/store instruction. In fact, the continuous or regular memory access patterns are defined in the wide/banked-memory to accelerate the load and store instructions.

As mentioned earlier, the length of vector processor is limited. In the practical implementation, the data lengths are usually greater than the Maximum Vector Length

(MVL) so that strip mining solution is proposed. Assume that the data length is $N > MLV$, to process this data vector in a parallel manner, first a loop is made to handle the MLV elements. Then, another loop is generated to process the $N \bmod MLV$ elements.

Vectorized operation within the conditional statement (*if*) cannot be done; therefore Vector Mask Registers (VMRs) are used to store the test results for the next use. Generally, the Vector processors have multiple pipelines of different types. Sometimes, the output of one pipeline instruction can be directly released into another pipeline. This technique is called chaining, to eliminate the intermediate storage between two pipelines. [45] For instance, in the following example, it can be seen that the output vector V1 is released to the next instruction:

MULV.D V1, V2, V3
ADDV.D V4, V1, V5

In some of the vector processors, special scatter, gather and masking instructions are used to process the sparse matrices efficiently. All these optimization makes the vector processors extremely faster and more efficient. [46]

3.4.5. Power Consumption

In order to evaluate the power consumption of the vector processors, there are some parameters which effect the power consumption. The first point is that there is trade-off between parallelism and power, the more parallelization, the less power is consumed. The simpler instruction and logic for execution large number of operation leads to lower power usage. In this way, there should not be multiple issues or dynamic operation logic as the process would become complicated and the power consumption increases. It has also been found that conditional execution results in further power saving.

By taking into account all the above mentioned methods, namely, optimization schemes and power consumption tips, we can optimize the vector processor performance as much as possible, which leads to lower power consumption and much more efficient performance while fulfilling the requirements.

3.5. Single Instruction Multiple Data

SIMD is a parallelism architecture which exploits data parallelism as opposed to the VLIW where the parallelism is used in the instructions. This technique has been added to the general purpose DSP and multimedia processors to afford a power efficient method of parallel processing.

The SIMD can be described as an architectural feature which includes a set of instructions that can speed up an application performance by allowing basic operation to be performed on multiple data elements in parallel with fewer instructions. By this means, the main difference between SIMD and vector processing is in the way that data elements are fed; in SIMD a stream of data elements are processed. However, it can be

said that vector processing machines apply the operation on the vector one element at a time through the pipeline processors, while the SIMD machines process all the element of the stream, simultaneously. In other words, the vector processors are SIMD operations. Figure 12 shows the capability of the SIMD processor that the execution units can be divided so that a single instruction is issued to be executed in on many ALU units, simultaneously.

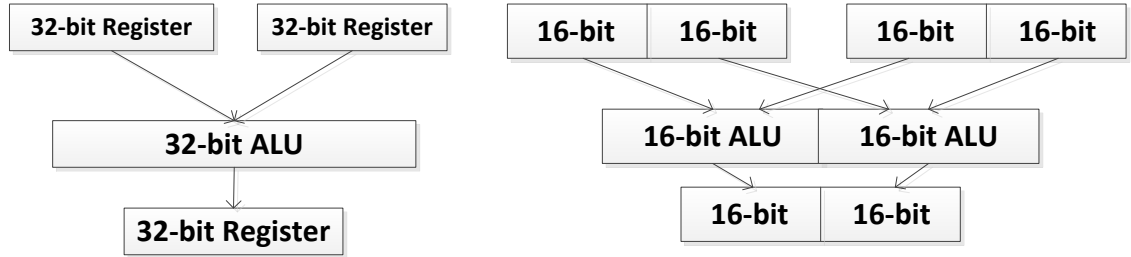


Figure 12. Execution units split in SIMD

The main limitation of the SIMD solution is that no mask register is available for the conditional statement. In the meantime, it suffers from the lack of sophisticated addressing mode, while in the vector processing scatter-gather and stride instructions are used. In the end, the number of operands is encoded into the operation code.

3.6. Vector Processors Deployment in Baseband Processing Wireless Modems

Due to the fact that almost all of the conventional modems functionalities are implemented in semiconductor, they are not configurable. On the other hand, these modems have not been designed to be configurable as they have been designed as application-specific systems, without general programmability, i.e., they contain a lot of fixed-function systems. Due to these reasons, those types of modem are called “*fixed-function modem*”. The challenges are increasingly coming into design, fabrication, planning and testing when the complexity and number of air interfaces rise. [47]

The wireless protocols and bands require significant resources to design and verify modern modems; therefore, more carrier specific modes and regions need to be accommodated. As a result, the conventional hardware modem designs are assumed expensive, large and complex.

On the other hand, due to the rapid growth and popularity of handheld devices working based on Wi-Fi/WLANs, the wireless standards are evolving at a rapid pace. By releasing new wireless interface standards, the traditional modems need costly and time consuming silicon redesign and spin to accommodate the new specifications in spite of the fact that they are limited in the terms of flexibility and adaptability.

In addition, the old fashion modem design implement discrete fixed function blocks for each supported connectivity protocol can result in a larger die sizes and higher pow-

er consumption. Consequently, the conventional fixed function modems, with their lengthy design cycles, requirement for discrete fixed function hardware and lack of adaptability requires the chips that are larger, inefficient, expensive and complex.

The limited compatibility of the fixed function modems leads to less competitive products. The users experience less optimal performance, expensive devices and fewer choices. Meanwhile, the network providers have to yield lower device performance and increased network capital expenditure costs.

The new wireless communication standards include new specifications, which result in more complexity in System-on-Chip (SoC) implementation. Therefore, relying on the sequential processors is not practical anymore. One technique to improve the flexibility, compatibility and adaptability of the baseband modems is the usage of processors with a specific application to replace the fixed function units. For example, utilizing the vector processors or SIMD processors is beneficial in term of cost. The applicability of the SIMD processors is feasible due to the fact that in the baseband processing modem, some of the data processing can be done in parallel. In fact, the baseband signal processing in the wireless modem contains such data parallelism, in principle. [48]

3.7. ConnX BBE32 DSP Core

As mentioned earlier, the incompatibility features of the ASIC baseband processing platforms with the evolving standards, fast time-to-market and long platform lives has brought the significance of the configurable DSP core to a higher level.

One particular VLIW machine is ConnX BBE32 which is a specific application processor for the next generation of baseband processors like LTE advanced, 4G cellular networks and multi-standards broadcast transceivers will be studied. Primarily, for such applications, high efficient computational cores are required to have high degree of parallelism in architecture. The ConnX BBE32 is built around the baseline Xtensa RISC architecture which implements a rich set of generic instructions optimized for efficient embedded processing. The power of the ConnX BBE32 comes from a comprehensive set of over 350 DSP and baseband optimized instructions excluding the baseline Xtensa RISC instructions. Hence, it can be summarized that the ConnX BBE32 is built on Tensilica's proven Xtensa LX customizable processor architecture, and is specifically designed to support the needs of software-based baseband processing.

The BBE32 DSP is 4-way VLIW processor, which contains vector processing and SIMD-extensions. This DSP engine fulfills the mentioned requirements by combining a 16-way Single Instruction Multiple Data (SIMD), 32 Multiplier-ACcumulators (MAC), 4-slot VLIW processing pipeline with a rich and extensible interfaces. It constitutes two groups of memories, Instruction (I-RAM) and Data (D-RAM0, D-RAM1) memories, for higher efficiency. [50]

BBE32 contains a comprehensive toolset of softwares such as high performance C/C++ compiler with automatic vectorization to support the VLIW pipeline. This processor is capable to execute four operations in parallel in every cycle; such massive op-

erations require high memory bandwidth which is provided through inserting two Load Store Units (LSUs). From power consumption point of view, this processor goes well beyond the conventional DSP cores.

Figure 13 demonstrates the ConnX BBE32 architecture in details. As it can be seen, the ConnX BBE32 utilizes variable length instructions of 96-bits for four operations in VLIW that may be executed in parallel. Moreover, the memory port is 96-bits and such units are fetched from the instruction memory in a memory cycle.

Fundamentally, BBE32 comprises of a set of pipelined execution units that provide flexible real and complex multiply-add, bitwise manipulation, data shift and normalization, data select, shuffle and interleave which make it very useful and attractive for the baseband processing modem applications. In order to obtain higher efficiency, it is feasible to fetch the instructions from the local instruction memory (IRAM). It is also capable to read from and write to the system memory and devices attached through the standard systems buses.

The ConnX BBE32 provides 4 VLIW instruction slots which are available for different operations. For instance, the instruction slot-0 is mainly used for load and store operation, the slot-1 only provides load operations via LSUs. The slot-2 mostly allows the ALU with multiply operations whereas slot-3 is solely available for the ALU operations present in the ConnX BBE32 instruction set. One of the interesting properties in the BBE32 is that by using the provided optional vector instruction extension and acceleration units such as division and FFT can be added into the basic BBE32 configurations. It is worth mentioning that these optional instruction exertions are design time parameters so that they cannot be changed once the processor is implemented in the chip. Thus, this core finds more adaptability and flexibility into the new WLANs standards and cellular networks. [50]

The compatibility of the ConnX BBE32 to the baseband signal processing modems becomes crystal clear by the fact that supported multi operations are applicable on the real and complex numbers, both. However, multiply-add, multiply-round, conjugate arithmetic and magnitude computations, full precision arithmetic are also provided. [48]

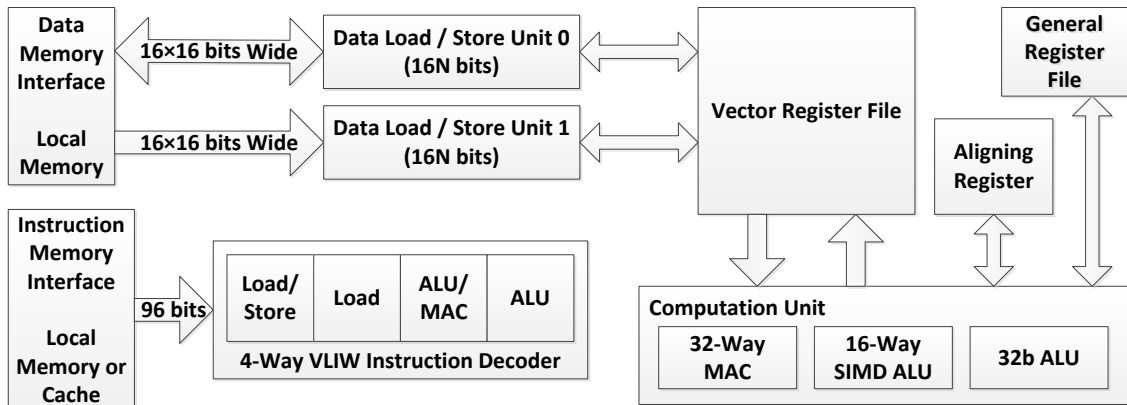


Figure 13. ConnX BBE32 architecture

Due to the specific applications that the processor is designed for, ten optional packages are considered to be supported which lead to the processing acceleration, as following:

- Aligning Load and Store package,
- 8-way integer and fractional vector divide package
- 16-way vector reciprocal square root package
- Bit-multiplication support for LFSR application and convolutional encoding
- 3-GPP soft-bit demapping package
- FIR package
- Symmetric FIR package
- Pairwise real multiply package
- FFT package
- Linear block decoder package

By the provided packages, especially FFT and FIR ones, the baseband signal processing would be easier.

It is worth mentioning that Tensilica has provided two different processor configurations, namely Low-Power (LP) and Performance-Maximized (PM) which are used in this research. Basically, the LP version of the ConnX BBE32 has only the base ConnX BBE32 instruction sets. The PM configuration includes all ten optional packages/accelerators instructions which are available in Xtensa Xplorer for ConnX BBE32 [50].

In addition to the optional packages, the ConnX BBE32 has a categorized set of the register files to deliver larger bandwidth and lower memory traffic. The first one comprises of sixteen 256-bit general purpose narrow vector registers (*vec*) capable of keeping operands and SIMD operations results. The second set consists of four 640-bit wide vector registers (*wvec*). Principally, the interface between the data memories the wide vector registers takes place through the narrow registers. In addition to the mentioned vector registers, other kind of optional registers are provided in the BBE32, which are helpful in flexibility and VLIW application, namely, Boolean vectors, Alignment registers and variable Shift/Select registers. [50, 51]

4. IEEE802.11AC TRANSMITTER IMPLEMENTATION

Through this chapter, the detailed data structure defined by the IEEE standard will be reviewed. In addition, the desired transmission scenario's requirements including the antenna configuration, modulation scheme, coding rate and bandwidth will be defined. Moreover, the implementation procedure for each transmission mode will be described, as well. It shall be mentioned that in the following chapter, the draft version of IEEE802.11ac standard has been followed in this research [52].

4.1. Data Structure

In this project, the transmitter is designed in such a way to support the desired operating points. As mentioned earlier, our main focus is on the PHY layer implementation of the IEEE802.11ac standard rather than the MAC specifications.

According to the standard definition, the VHT packet structure is composed of three parts. The first part is the legacy preamble, the second one is the VHT preamble, and the last one is the data part. Figure 14 illustrates the VHT packet structure. The legacy portion consists of the several fields, namely, L-STF, L-LTF and L-SIG, which are described in the following. The VHT part also includes the VHT-SIG-A, VHT-SIG-B, VHT-STF and VHT-LTF fields. Table 2 defines each field. [52]

As the frequency domain processing of the VHT-SIG-B field of the preamble part and the data field is performed on the DSP, the study is mainly carried out for these two fields.

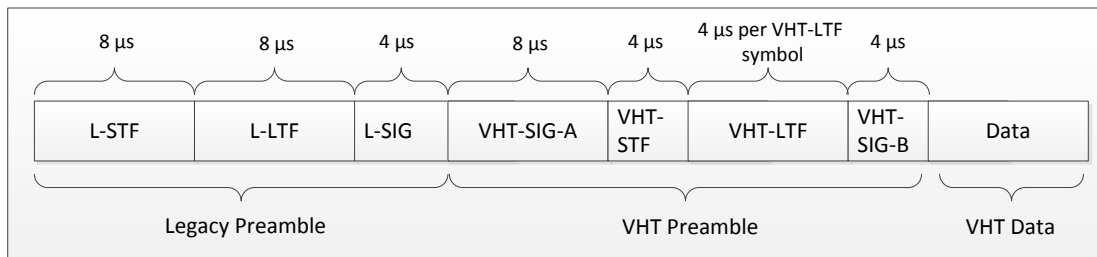


Figure 14. VHT packet structure

Table 2. *VHT packet fields*

Field	Description
L-STF	Non-HT Short Training field
L-LTF	Non-HT Long Training field
L-SIG	Non-HT SIGNAL field
VHT-SIG-A	VHT Signal A field
VHT-STF	VHT Short Training field
VHT-LTF	VHT Long Training field
VHT-SIG-B	VHT Signal B field
Data	The Data field carries the PSDU(s)

4.1.1. Legacy Preamble

The first part of the VHT packet structure consists of legacy (non-VHT) training fields. Furthermore, each field is described in details, as follows.

The Legacy Short Training Field (L-STF) is used for the start of the packet detection and Automatic Gain Control (AGC) setting. It is also utilized for the initial frequency offset estimation and initial time synchronization.

As shown in Figure 11, the L-STF length is $8\mu\text{s}$, which actually includes ten repetitions of a $0.8\mu\text{s}$ symbol, in the time domain. In the standard, the L-STF is defined based on the frequency domain sequences which are different for each transmission bandwidth.

The Legacy Long Training Field (L-LTF) is also an $8\mu\text{s}$ length training field, which is used for channel estimation, more accurate frequency offset estimation, and time synchronization.

L-LTF is composed of two $3.2\mu\text{s}$ long training symbols with a $1.6\mu\text{s}$ cyclic prefix. Similar to the L-STF, depending on the used transmission bandwidth, the L-LTF sequences are defined in a different manner.

L-SIG is signal field consisting of 24 information bits about the transmission rate and information length.

As L-SIG elements are bits, the L-SIG itself is transmitted using BPSK modulation scheme and coding rate of $1/2$ binary convolutional code. The significance of the L-SIG is not only because the desired receivers decode the L-SIG properly, but also because the nearby STAs accurately defer the channel access.

It is composed of a $4\mu\text{s}$ symbol and depending on the channel bandwidth the number of subcarriers and the length would be different.

4.1.2. Very High Throughput Preamble

VHT preamble of the VHT packet structure begins with VHT-SIG-A and continues with VHT-STF, VHT-LTF and VHT-SIG-B.

VHT-SIG-A field carries the required information to interpret VHT PPDU. VHT-SIG-A field consists of two parts, namely VHT-SIG-A1 and VHT-SIG-A2; each of which consists of 24 bits. VHT-SIG-A1 is transmitted before VHT-SIG-A2.

VHT-SIG-A totally contains 48 bits carrying the information related to the bandwidth, number of space time streams, transmit beam forming, modulation and coding scheme, and the guard interval type (short/long).

The signaling part of VHT waveform will be started by the VHT Short Training Field (VHT-STF). By receiving this field, we switch onto the cyclic shift diversity table which is specifically defined for VHT preamble fields.

The main purpose of the VHT-STF field is to improve the automatic gain control estimation in a MIMO transmission. The duration of the VHT-STF field is 4 μ s. The frequency domain sequence is used to construct the VHT-STF field in a 20 MHz transmission which is identical to the L-STF field. In a 40 MHz and an 80 MHz transmission, the VHT-STF field is constructed from the 20 MHz version by frequency shifting a duplicate of it to each 20 MHz subchannel and applying appropriate phase rotations per 20 MHz subchannel.

VHT Long Training Field (VHT-LTF) is conceptually similar to the HT-LTF with some new sequences for wider channel bandwidths 80MHz and 160MHz. By this means, the construction procedure has these two main differences: the first one is the presence of up to 8 spatial streams, and the second is allowance for phase tracking during VHT-LTF. It is a 4 μ s frame per VHT-LF symbol.

The VHT-LTF provides a means for the receiver to estimate the MIMO channel between the set of constellation mapper outputs (or, if STBC is applied, the STBC encoder outputs) and the receive chains. It should be noted that the channel estimation is done by using the pilot subcarriers inserted into the VHT-LTF symbols.

Although the primary purpose of using VHT-SIG-B is for signaling user specific information in a MU packet, it is still used in all packets to maintain an unified preamble format for VHT packets. However, in SU scenario, the receiver does not need to process VHT-SIG-B. Since VHT-SIG-B is coming after VHT-STF and VHT-LTF, it is formed differently than VHT-SIG-A in such a way that in our system the bits are repeated including the tail bits. By this means, the processing gain at the receiver is obtained by averaging repeated soft values at the decoder input.

As shown in Figure 14, VHT-SIG-B is a 4 μ sec OFDM symbol with single stream, BPSK, BCC rate 1/2 modulation. In our systems, the channel bandwidth is 80MHz which means there are 29 bits available in VHT-SIG-B consisting of 23 information bits and 6 tail bits, each repeated four times, with a single pad bit appended at the end.

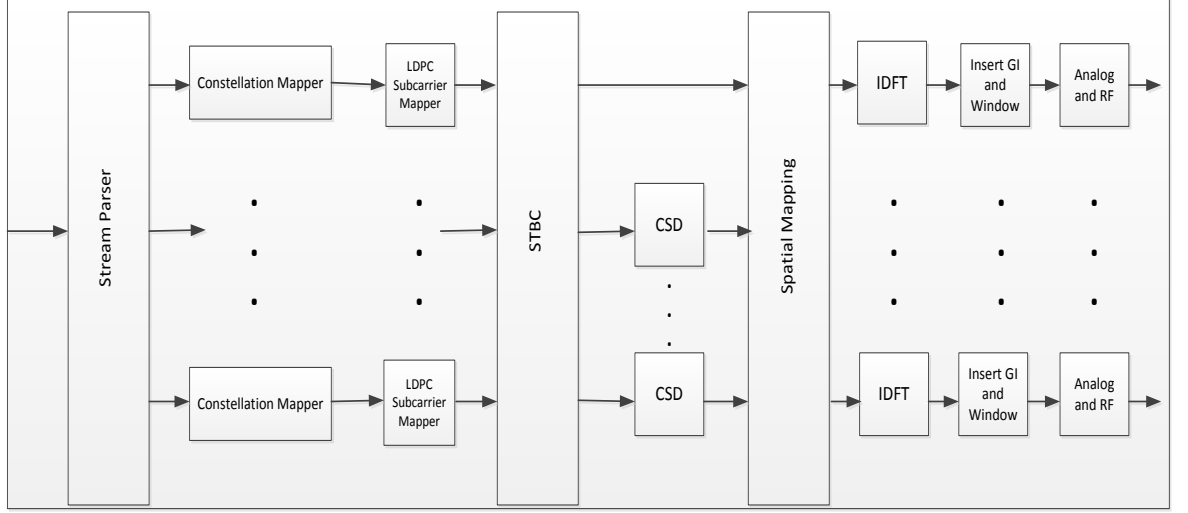


Figure 15. Principal processing block diagram for VHT data field

4.1.3. VHT Data Field

The construction of the data field, in a VHT SU PPDU with LDPC encoder, proceeds as shown in Figure 15. The operational mechanism of each block is explained in the following.

4.1.3.1. Stream Parser

After coding and puncturing, the data bit streams at the output of the FEC encoders are processed in groups of N_{CBPS} bits. Each of these groups is re-arranged into N_{SS} blocks of N_{CBPS} bits. In the case of MU transmissions, the rearrangements are carried out in the same way per user. [37]

The number of bits assigned to a single axis (real or imaginary) in a constellation point in a spatial stream is denoted by the equations (4.1), (4.2), and (4.3):

$$s = \max \left\{ 1, \frac{N_{BPSCS}}{2} \right\} \quad (4.1)$$

$$N_{Block} = \left\lfloor \frac{N_{CBPS}}{N_{ES} \cdot S} \right\rfloor \quad (4.2)$$

$$M = \frac{N_{CBPS} - N_{Block} \cdot N_{ES} \cdot S}{S \cdot N_{ES}} \quad (4.3)$$

where N_{CBPS} , N_{BPSCS} , N_{ES} , N_{Block} are the Number of Coded Bits per Symbol, Number of Coded Bits per Subcarrier per Spatial stream, Number of BCC encoder, and the Number of Blocks, respectively.

Consecutive blocks of s bits are assigned to different spatial streams in a round Robin fashion. Therefore, S bits from the output of the FEC encoder would be divided among the spatial streams so that each stream would have s bits. Then the next S bits

from the output of the encoder are used, at some point if the number of the N_{CBPS} is greater than $N_{Block} \cdot N_{ES} \cdot S$, then the last $N_{CBPS} - N_{Block} \cdot N_{ES} \cdot S$ bits of each OFDM symbol are provided by taking $M \cdot s$ bits from the output of the first encoder. By this means, each stream (streams 1 to M) would take s bits, in continuation $M \cdot s$ bits from the output of the next encoder are used to feed the spatial stream $M + 1$.

4.1.3.2. Constellation Mapper

The OFDM subcarriers shall be modulated by using BPSK, QPSK, 16-QAM, 64-QAM, or 256-QAM, depending on the data rate requested. The encoded and interleaved binary serial input data shall be divided into groups of N_{BPSC} (1, 2, 4, 6, or 8) bits and converted into complex numbers representing BPSK, QPSK, 16-QAM, 64-QAM, or 256QAM constellation points, respectively. The conversion shall be performed according to Gray-coded constellation mappings with the input bit b_0 being the earliest in the stream. The output values d are formed by multiplying the resulting $(I + jQ)$ value by a normalization factor $KMOD$ (which depends on the base modulation mode), defined as follows:

$$d = (I + jQ) \times KMOD. \quad (4.4)$$

It should be noted that modulation type can differ from the start to the end of the transmission, as the signal changes from SIGNAL to DATA. However, in case of using 256-QAM modulation, a normalization/scaling factor should be used which is $\frac{1}{\sqrt{170}}$.

4.1.3.3. Low-Density Parity Check Tone Mapper

The LDPC tone mapping shall be performed on all LDPC encoded streams as described in the chapter 2 by using an LDPC tone-mapping distance parameter D_{TM} . D_{TM} is constant for each bandwidth and its values for different bandwidths are shown in Table 3. LDPC tone mapping shall not be performed on streams that are encoded using BCC.

Table 3. LDPC tone mapping distance for different bandwidth

Parameter	20MHz	40MHz	80MHz	160 MHz, 80+80 MHz
D_{TM}	4	6	9	9

The objective of the LDPC tone mapper is to map consecutive OFDM symbols to non-consecutive subcarriers. It is worth noticing that LDPC tone mapping is done per OFDM symbol.

LDPC tone mapping is done by altering the incoming streams of complex numbers from the constellation mapper; meaning, it shuffles the data subcarriers in each OFDM symbol in each stream of complex numbers. The equation (4.5) presents how LDPC tone mapper works:

$$d'_{t(k),i,n,l,u} = d_{k,i,n,l,u} \quad (4.5)$$

where l is zero for 80MHz transmission, u is the user number, i is the index of spatial streams, k is the number of complex data numbers per frequency segment which is 234, and n is the number of symbols. According to the parameters values, $t(k)$ can be calculated by using equation (4.6):

$$t(k) = D_{TM} \left(k \bmod \frac{N_{SD}}{D_{TM}} \right) + \left\lfloor \frac{k \times D_{TM}}{N_{SD}} \right\rfloor. \quad (4.6)$$

By doing the above operation, each two consecutively generated complex constellation numbers would be mapped into two data tones which are at least $D_{TM} - 1$ far from other data tones.

4.1.3.4. Space Time Block Coding

This subsection defines a set of optional robust transmission techniques that are applicable only when using STBC coding for VHT SU PPDU. In this case, $N_{SS,0}$ spatial streams are mapped to $N_{STS,0}$ space-time streams. These techniques are based on STBC. When the VHT-SIG-A STBC field is 1, a symbol operation shall occur between the constellation mapper and the spatial mapper. In other words, when the number of the spatial streams is lower than the number of space time streams, the STBC technique is used.

It can be said that Space Time Block Coding is performing similarly to diversity methods and it is capable of providing same diversity gain as maximal combining ratio. Depending on the number of the spatial streams (N_{SS}) and the number of the space time streams (N_{STS}), the output of the constellation mapper would be coded as the following table:

Table 4. STBC input and output symbols

N_{STS}	N_{SS}	i_{STS}	$\tilde{d}_{k,i_{STS},2m,0}$	$\tilde{d}_{k,i_{STS},2m+1,0}$
2	1	1	$d_{k,1,2m,0}$	$d_{k,1,2m+1,0}$
		2	$-d_{k,1,2m+1,0}^*$	$d_{k,1,2m,0}^*$
4	2	1	$d_{k,1,2m,0}$	$d_{k,1,2m+1,0}$
		2	$-d_{k,1,2m+1,0}^*$	$d_{k,1,2m,0}^*$
		3	$d_{k,2,2m,0}$	$d_{k,2,2m+1,0}$
		4	$-d_{k,2,2m+1,0}^*$	$d_{k,2,2m,0}^*$

It is worth noticing that when STBC is applied, an odd number of space time streams is not allowed, and the following relation (4.7) shall be established:

$$N_{STS,0} = 2N_{SS,0}. \quad (4.7)$$

4.1.3.5. Pilot Insertion

According to the channelization presented in the chapter 2, for a 20 MHz transmission, four pilot tones shall be inserted in subcarriers $K \in \{-21, -7, 7, 21\}$. For a 40 MHz transmission, six pilot tones shall be inserted in subcarriers $-53, -25, -11, 11, 25$, and 53 .

For an 80 MHz transmission mode, eight pilot tones shall be inserted in subcarriers $\{-103, -75, -39, -11, 11, 39, 75, 103\}$. The pilot mapping P_n^k of subcarrier k of symbol n shall be specified based on the following equations:

$$P_n^{\{-103, -75, -39, -11, 11, 39, 75, 103\}} = \{\psi_{n \bmod 8}, \psi_{(n+1) \bmod 8}, \dots, \psi_{(n+7) \bmod 8}\} \quad (4.8)$$

$$P_n^{k \notin \{-103, -75, -39, -11, 11, 39, 75, 103\}} = 0 \quad (4.9)$$

where ψ_m is defined according to table 5:

Table 5. Pilot values for 80MHz transmission bandwidth

ψ_0	ψ_1	ψ_2	ψ_3	ψ_4	ψ_5	ψ_6	ψ_7
1	1	1	-1	-1	1	1	1

In addition to these pilot subcarriers, 14 null subcarriers shall be inserted into the data streams resulting in data streams containing 256 subcarriers.

4.1.3.6. Cyclic Shift Diversity

Cyclic shift diversity is applied to each OFDM symbol separately in order to decorrelate the transmitted signals from different antennas and prevent from bad beam forming effects. Based on the number of the space time streams, T_{CS} would be applied to the OFDM symbols according to the equation (4.10):

$$S_{cs}(f) = S(f)e^{-j2\pi f T_{CS}}. \quad (4.10)$$

Table 6. Cyclic shift values for data field packets

Spatial stream	1	2	3	4
1	0 ns	-----	-----	-----
2	0 ns	-400 ns	-----	-----
3	0 ns	-400 ns	-200 ns	-----
4	0 ns	-400 ns	-200 ns	-600 ns

The time shift is equivalent to a phase rotation in the frequency domain, as it has been shown in the previous formula; cyclic shift diversity can be done by multiplication of an exponential function.

4.1.3.7. Spatial Mapping

Depending on the number of space time streams and the transmit chains, transmitter may rotate/scale the constellation mapper/STBC output. The scaling factor is the square root of the number of space time streams, and the rotation is done with the help of Space Time Block Coding (STBC).

4.1.3.8. Phase Rotation

According to the standard, for each transmission bandwidth there is a gamma function which makes a rotation in tones. In 80MHz transmission, function $\gamma_{k,80}$ is as the equation (4.11):

$$\gamma_{k,80} = \begin{cases} 1, & k < -64 \\ -1, & k \geq -64 \end{cases} \quad (4.11)$$

As it can be realized from the equation, phase rotation is only multiplication by +1/-1 depending on the subcarrier indices.

4.2. Transmission Scenarios

In the following sections, the desired transmission points to be covered are described. With reference to Figure 12, the operational blocks from the stream parser to IFFT are implemented in this project for all the following transmission modes.

4.2.1. Case a: 2x2 SU-MIMO Transmission

In the first transmission mode, a contiguous 80MHz bandwidth is used to communicate through the wireless channel. The usage of two spatial streams in a 2x2 antenna configuration means that the Space Time Block Coding (STBC) block does not need to be employed. Figure 16 shows the implementation of the first case block diagram. In this scenario, the target data rate is 780Mbps by having a 2x2 MIMO antenna, 256QAM modulation scheme with coding rate of 3/4.

As mentioned earlier, in 80MHz channel bandwidth, the FFT size is 256 so that each OFDM symbol includes 256 subcarriers to carry the data. In the implementation procedure, it has been found that the transmission can be done in a different order as it is easier to deal with bits rather than the complex number. For instance, although the STBC coder and LDPC tone mapper are defined to be executed after the constellation mapper, they can be also implemented for the bits. Therefore, the implementation procedure is different than the shown block diagram.

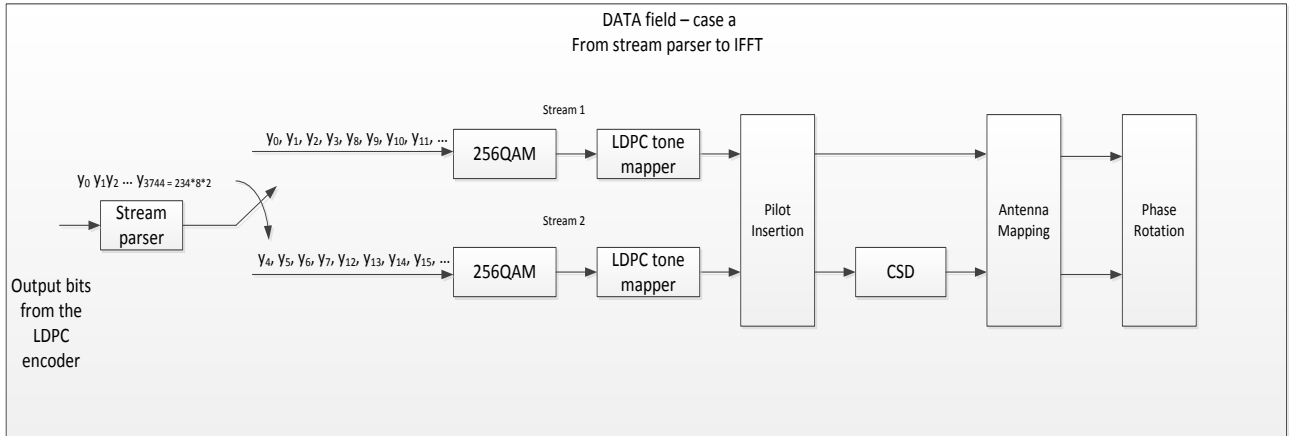


Figure 16. Principal block diagram of Case a

At the beginning, an additional block called preparation block is used to rearrange the incoming bit streams to become ready for LDPC tone mapping and modulation. As for the processor is 16-bits, the preparation block rearranges the data in the frames of 16-bits. The incoming bit stream has $234 \times 8 \text{ bits}$, and has the following format. From left to right, the first and second 4 bits actually present the real part of the first and second streams (first subcarrier), respectively. In the meantime, the third and fourth 4 bits show the first and second streams imaginary parts (first subcarrier), correspondingly. Therefore, the preparation block combines the real and imaginary parts of each subcarrier in such a way that the first outcoming 16-bits frame has the real parts of two streams, and the second 16-bits frame has the imaginary parts (8 bits in both frames are zero). Then, two streams of complex numbers are ready to be fed into the LDPC tone mapper.

In the LDPC tone mapper, the data subcarriers of both streams are shuffled at the same time. According to the provided information in section 4.1.3.3., LDPC tone mapper alters the subcarriers' location of each OFDM symbol in each stream. It is worth of noticing that the incoming data streams are aligned to 32 bytes which means streams of complex numbers with $240 \times 8 \text{ bits}$ are processed, although the original number of data subcarriers is 234.

It has been found that if the stream parser and constellation mapper are combined, the performance would be most optimized. Therefore in the third phase, the LDPC tone mapped streams of complex numbers are parsed and mapped into the constellation mapper, simultaneously. As explained earlier, streams parser parses $2 \times 240 \times 8$ coded bits per symbol (N_{CBPS}) between two streams that means each stream would have 240×8 coded bits per symbol, meaning, each stream has 8 bits including 4 bits for real part and 4 bits for the imaginary part. By using 256-QAM modulation, every 8 bits are simultaneously mapped into one 256-QAM constellation point.

According to the specifications given in section 4.1.3, all the functions after the LDPC tone mapper including pilot insertion, Cyclic Shift Diversity (CSD), spatial map-

ping and phase rotation are originally based on multiplication between the data subcarriers and coefficients. Due to this reason, they can be merged into one block and executed in one operation. Consequently, the outcoming streams from the stream parser and constellation mapper block will be processed in one block to be ready for the IFFT operation. For this purpose, we created a look up table including all those numerical values resulted from the mentioned operations to be multiplied by the data subcarriers. There are several remarkable points, the first one is that due to the existence of two space time streams, the spatial mapping is only a scaling operation with the scaling factor of $\frac{1}{\sqrt{2}}$. The second one is originated from the repetitive nature of the cyclic shift diversity values for the data subcarriers meaning the CSD table is duplicated for every eight subcarriers. The last point but not the least is that the first stream remained unchanged while the second one is shifted by 400ns in the time domain under the CSD operation.

4.2.2. Case b: 4x4 SU-MIMO Transmission

Similar to the previous case, the usage of 80MHz bandwidth provides 256 subcarriers to send the data. In addition, transmission of four spatial streams through a 4x4 antenna configuration results in the data rate of 1560Mbps by having modulation scheme 256QAM with coding rate of 3/4. It is worth mentioning that the equal number of spatial streams and the space time streams, STBC is not employed. The transmission block diagram for this case is shown in Figure 17.

Due to the fact that the processor is 16-bits, the incoming bits streams shall be rearranged. But in this case, as 4 spatial streams are used, the first incoming 16 bits already feature the real part of the first subcarrier of each stream, and the second 16 bits are the imaginary parts. By this means, the desired 16-bits packets are ready so that no preparation is needed and the bit streams can be directly fed into the LDPC tone mapper.

According to the standard, the LDPC tone mapper maps the OFDM symbols into the other indices by a sufficient distance to avoid any distortion.

After shuffling the data bits in the LDPC tone mapping block, the stream parser allocates 8 bits to each stream and maps them into one constellation point, at the same time. Therefore, stream parser parses $4 \times 240 \times 8$ coded bits per symbol (N_{CBPS}) among four streams that results in each stream having 240×8 coded bits per symbol, meaning, each stream has 8 bits including 4 bits for real part and 4 bits for the imaginary part. By using 256-QAM modulation, every 8 bits are simultaneously mapped into one 256-QAM constellation point.

The rest of operation, namely pilot insertion, cyclic shift diversity, spatial mapping and phase rotation, similar to the previous case, are done by multiplication between the look up table numerical values and data subcarriers. The scaling factor for the spatial mapping operation would be $\frac{1}{\sqrt{4}}$, and the cyclic shift diversity in this scenario would make change in all the spatial streams except the first one. As a result, the first stream would be remained unchanged, but the second, third and fourth streams are shifted in

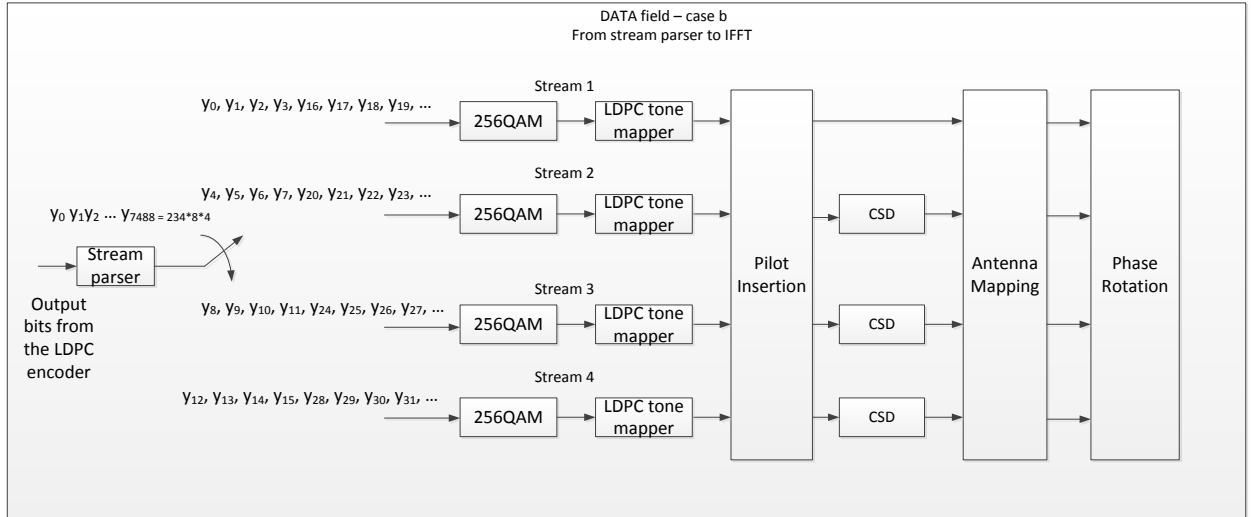


Figure 17. Principal block diagram of Case b

the time domain by 400ns, 200ns and 600ns respectively. The phase rotation is also a multiplication with $1/-1$ depending on the subcarrier index.

4.2.3. Case c: 2x2 Antenna Configuration with 1x1 SU-SISO Transmission

In this case, the application of 80MHz bandwidth, 256-QAM modulation scheme and 2x2 antenna configuration leads to 390Mbps data rate. The additional antenna is assumed to be used at both sides to achieve diversity gain. Here, the number of spatial streams is lower than the space time streams number which brings up the idea of employing STBC encoder. Figure 18 shows the transmission structure for the third transmission scenario.

Due to the unequal number of the spatial streams and space time streams, the STBC encoding method must be employed. We apply STBC in this step as it is easier to process the bits rather than the complex numbers. According to the STBC description (given in Table 22-20 in the standard specification), some symbols need to be conjugated i.e. the imaginary part should be negated and in bit level this only means inverting the sign bit for the imaginary part. For that reason, it is possible to do the STBC coding in the preparation block, as well. Consequently, in this block, the incoming stream of size 243×8 bits is duplicated and for some of them (depending on the index) the sign bit is changed. At the end, two streams of the size of 243×8 bits come out to be fed into the LDPC tone mapper.

After applying the STBC coding into the streams, LDPC tone mapper is applied in which the bit streams are interleaved or replaced into new data tones. By this means, the output is LDPC tone mapped STBC coded bit streams.

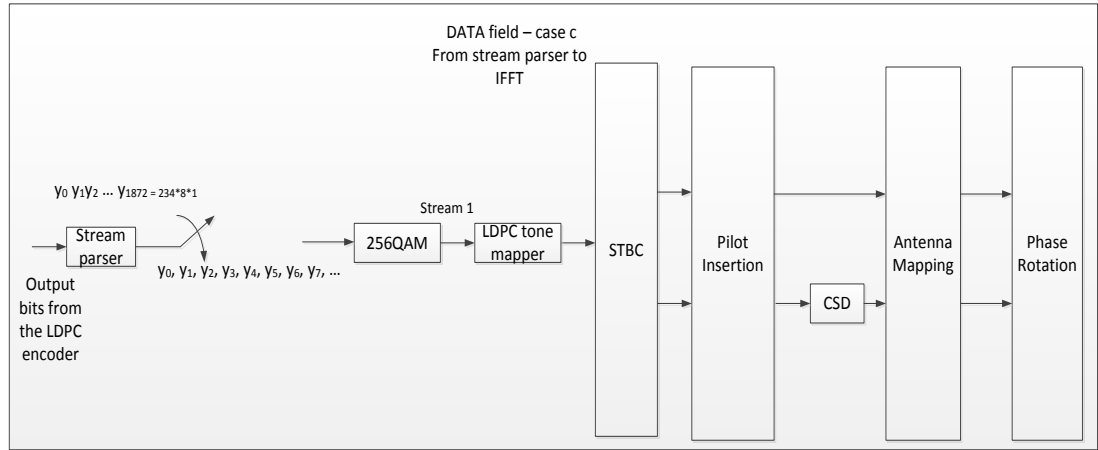


Figure 18. Principal block diagram of Case c

In the third phase, stream parser divided the bit streams into two space time streams at which each stream would have 243×8 bits. Meanwhile, every 8 bits are mapped into one 256-QAM constellation point.

In the last block, pilot insertion, cyclic shift diversity, antenna mapping (scaling) and phase rotation are done. In the cyclic shift diversity part, the second stream is only shifted by 400ns, and in the spatial mapping both streams are scaled by $\frac{1}{\sqrt{2}}$ and multiplied by $1/-1$ in the phase rotation step.

4.2.4. Case d: 4x4 Antenna Configuration with 2x2 SU-SISO Transmission

In this transmission mode, as depicted in Figure 19, the unequal number of spatial streams and space time streams means STBC coding must be employed. Under the specified circumstances, a data rate of 780Mbps is desired to be obtained while only two spatial streams are used to generate 4 space time streams to be mapped into a 4x4 antenna configuration. Similar to the previous case, the modulation scheme 256QAM with coding rate of $3/4$ is utilized with the presence of short GI.

To get the optimized performance in the processor, it is better to merge the STBC coding into the first block to be done along the preparation operation, at the same time. According to the specification, only the sign bit of the bit streams shall be changed and the rest of bits are just duplicated. Therefore, at the output of the STBC and preparation block, four space time streams of the size of 240×8 bits are ready to be LDPC tone mapped. Afterwards, the bit streams will be LDPC tone mapped, which means the sub-carriers indices will be changed.

Then the stream parser allocates 8 bits to each stream and constellation mapper maps them into one 256-QAM constellation point, simultaneously.

The rest of blocks are also done based on the multiplication between the subcarriers and look up table which includes all the numerical values of the mentioned operations.

In this case, the scaling factor is $\frac{1}{\sqrt{4}}$ in the spatial mapping stage. For the cyclic shift diversity, the first stream remained unchanged and the second, third and fourth streams are shifted by 400ns, 200ns and 600ns, respectively.

4.3. Time and Frequency Parameters

In order to design the OFDM symbols in well accordance to the IEEE802.11ac standard, specific parameters must be selected.

In this project, we have utilized a short guard interval of $0.4\mu\text{s}$ to be appended to the VHT data part whose duration is, as mentioned earlier, $3.6\mu\text{s}$ in case of using short guard interval (GI). The symbol interval (T_{SYM}) duration is dependent on the length of the guard interval, which is $3.6\mu\text{s}$ due to the usage of short GI in our design. Accordingly, the symbol rate ($1/T_{SYM}$) can be calculated by taking the inverse value of the symbol interval, which is almost 277ksps, in this case. The rest of the timing constant such as the duration of the legacy preamble and VHT preamble have already been described in the previous sections.

The channel bandwidth in all of the transmission scenarios is 80MHz. Independent of the channel bandwidth; the subcarrier frequency spacing is equal to 312.5 KHz. The total number of subcarriers carrying data, as the FFT size is 256, is 234 subcarriers, and the channelization details have been termed in the chapter 2. The rest of the subcarriers are null and pilot for channel estimation and equalization purposes.

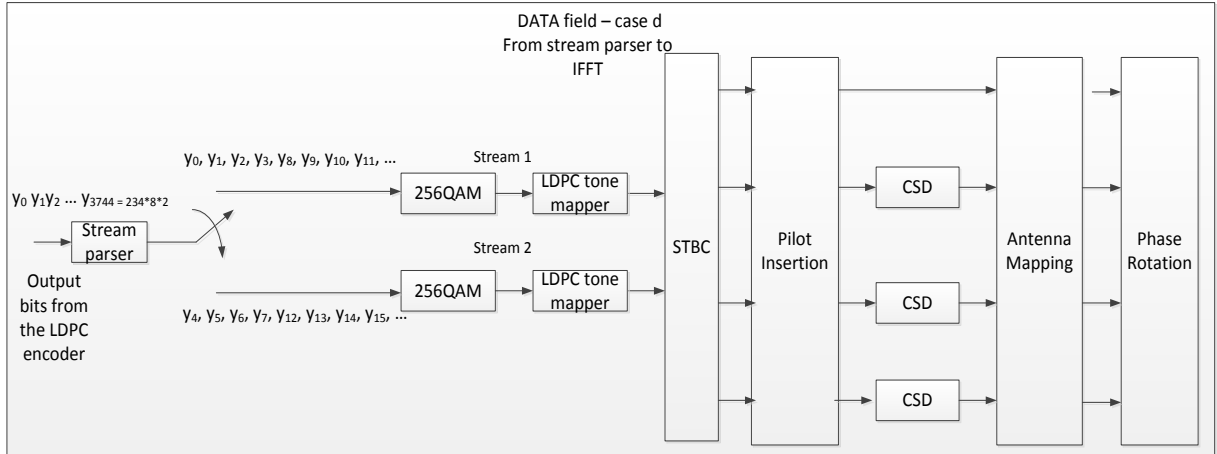


Figure 19. Principal block diagram of Case d

5. RESULTS AND ANALYSIS

This chapter includes the implementation results which are profiled in the terms of clock cycles, power and energy consumption and memory usage. In addition, the obtained results will be discussed and compared with some references.

5.1. Software Implementation

In order to program and evaluate the performance of the ConnX BBE32 DSP core, the Xtensa Xplorer (XX) integrated Development Environment (IDE) is used which is capable of providing a C/C++ software development workspace. It also offers a comprehensive collection of code generation and analysis tools. [51]

However, the utilized processor inherently provides a wide variety of the optimization approaches to make the software implementation efficient. As mentioned in the previous section, appropriate configuration and programming style play an important role in the efficiency of the implementation, thus some optimization techniques have been applied in this project to speed up the processing. In principle, everything has been optimized almost in machine level as the C-code is full of macros, which actually means that the code is not portable anymore. Another effective optimization approach was merging and combining the functions as much as possible. Specifically those functions whose functionality involves multiplication with a constant value, such as phase rotation, spatial mapping, pilot insertion and cyclic shift diversity. Moreover, since it is easier to deal with bits rather than complex numbers, we have implemented as many operations as possible before the constellation mapping. For instance, although in the standard and, as shown in Figure 15, the STBC and LDPC tone mapper blocks are defined to be employed after the 256-QAM modulation; it has been found that such operations can be efficiently implemented when the input data is still in bits and not yet modulated to symbols.

5.2. Clock Cycles

To evaluate the processor performance in the term of clock cycle, the instruction set simulator (iss) is used which determines the needed clock cycles for processing one OFDM symbol.

The FFT operation needs 311 and 250 clock cycles per OFDM symbol to be done in LP and PM models, respectively. Table 7 and Table 8 show the previous tables in the form of bar chart as it is easier to figure out the difference and making comparison.

The first transmission has the lowest number of clock cycles, since it has only two spatial streams without having STBC so that it is the simplest transmission scenario. In the second transmission scenario, as it was mentioned that the preparation block is not required be employed so that in Table 7 and Table 8, the preparation clock cycle is equal to zero. For the third case, as the number of spatial streams was lower than the number of space time streams the STBC encoder was used. Therefore, in the first block, in addition to the preparation, the STBC encoding results are reported, That is why the preparation bar is larger than the other cases.

Similar to the previous transmission mode, in the fourth transmission case, the unequal number of spatial streams and space time streams brought up the idea of using STBC. Consequently, the preparation bar shows both preparation and STBC operations result. However, due to the similar reason as the second mode, the preparation is not needed. That is why the number of clock cycles is lower than in the third operation mode, although the number of spatial streams is higher. The numerical values for all the transmission scenarios can be found in the Appendix 1.

It is worth noticing that exploiting the PM configuration leads to the lower number of clock cycles required to execute each transmission mode. As a matter of fact, the existence of the optional packages accelerates the processing procedure. However, the speedup is almost negligible, as the additional packages will add some hardware to the processor and speedup is one few percentages.

Table 7. Clock cycle results in LP model

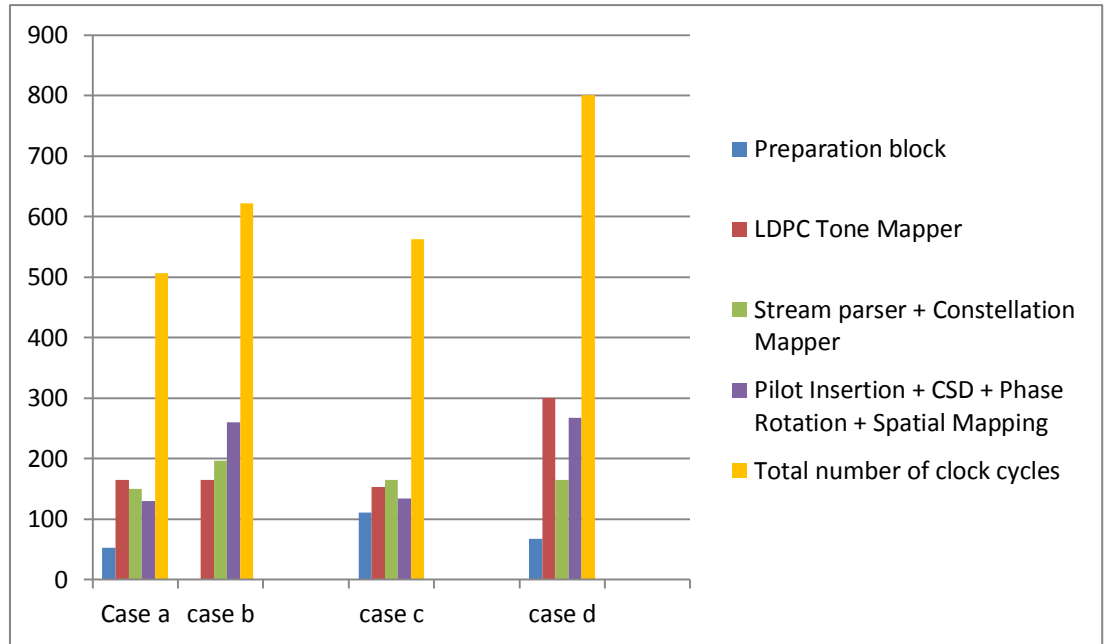
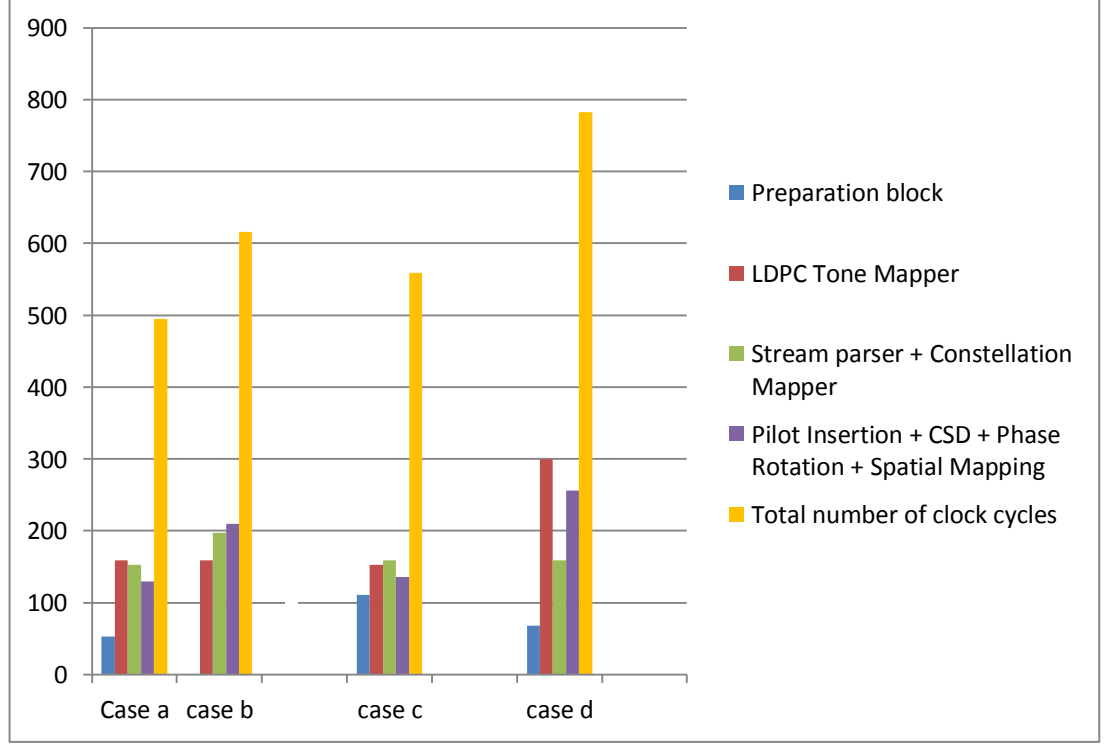


Table 8. Clock cycle results in PM model

5.3. Power Consumption

One of the most useful performance analysis factors is the power consumption which is, in this case, dependent on the memory configuration/capacity. As the Energy Xplorer tool is only able to analyze the energy for each function, first the energy is estimated and then the power consumption is calculated by dividing the energy values by time. The time for each block is different and calculated from the multiplication between the clock cycles and 2ns (the period of each clock cycle or the inverse of frequency). Although, the tool provides the total power consumption for each transmission scenario, it includes all the required power for initialization within the whole run-time.

As mentioned earlier, the memory configuration affects on the power consumption, so we have considered two common cases which are the maximum (128k) and half (64k) of the memory capacity. In order to analyze the energy consumption, the 40nm Low-Power IC technology provided by the vendor is used, and the operation frequency is assumed to be 500MHz. The monitoring time for the energy analysis is 3.6 μ s, and the estimated energy includes both leakage and dynamic parts. In the following, the related results to the power consumption for each function are reported for PM model, in case of full and half memory usage. The power consumption results for the PM model are not presented as they do not differ from the LP model results.

Table 9. Power consumption for each function of the transmission scenarios in mW, 128K

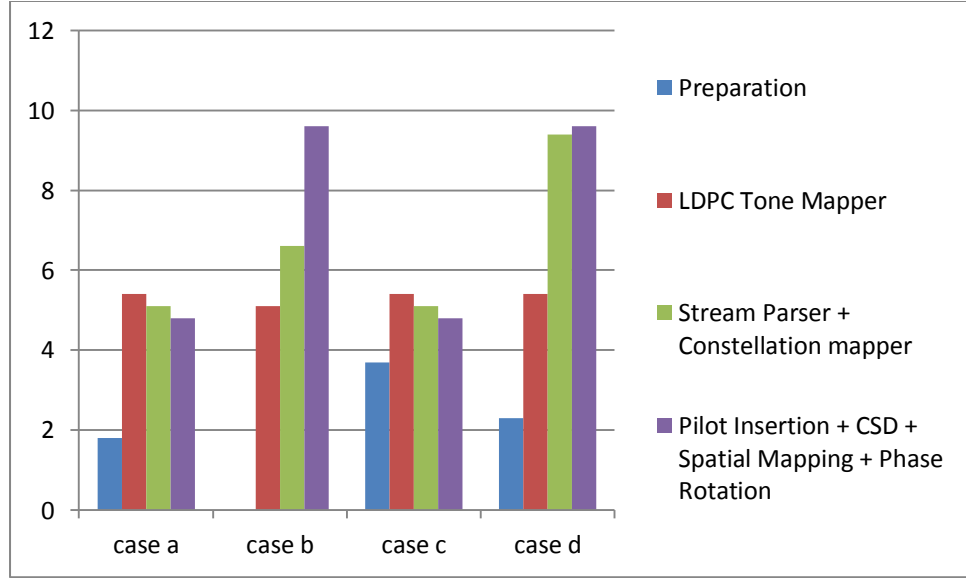
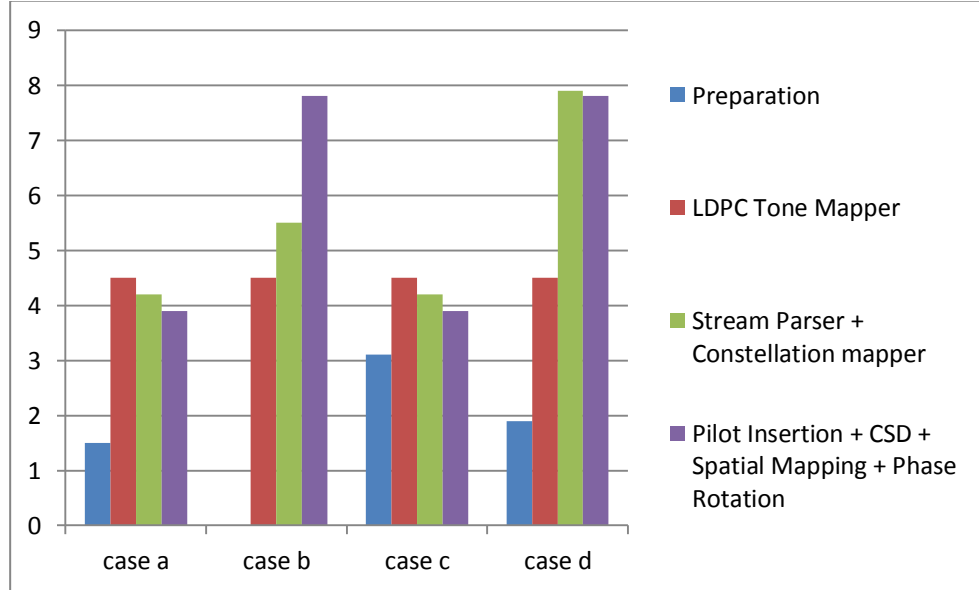


Table 10. Power consumption for each function of the transmission scenarios in mW, 64K



It can be concluded from the Table 9 and Table 10 that the second and fourth transmission scenarios have the highest rate of power consumption among the transmission cases which is due to the existence of four spatial streams for processing.

Table 11 presents the total power consumption for all the transmission scenarios profiled in the PM configurations and memory capacity of 128K. The same information is also introduced in Table 12 when the memory capacity is 64K.

Table 11. Total Power consumption [mW] for PM model in case of full memory

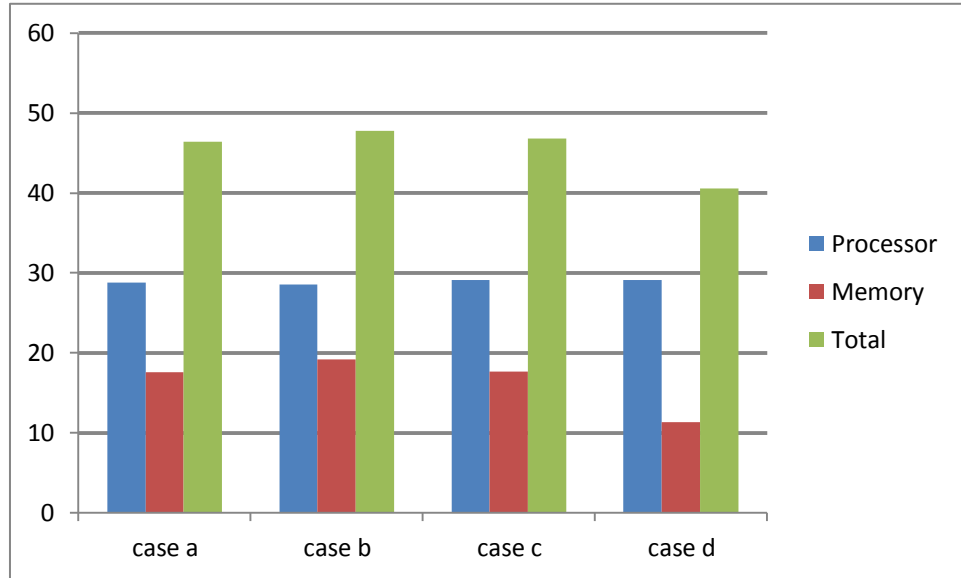


Table 12. Total Power consumption [mW] for PM model in case of half memory

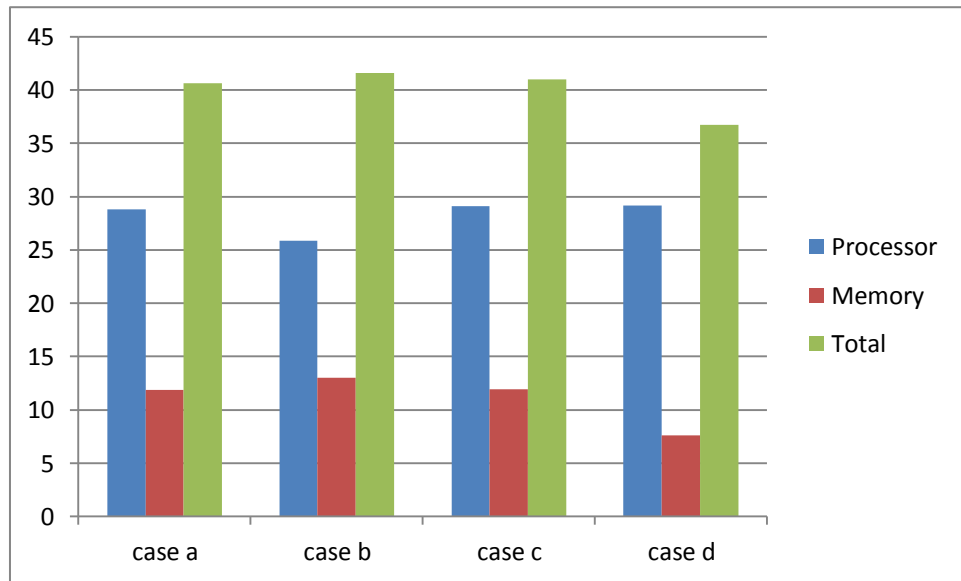


Table 13 and Table 14 show the total power consumption for all the transmission scenarios profiled in LP configurations for maximum and half capacity of memory, respectively. As it can be observed, the processor has the highest share in the total power consumption due to the fact that huge amount of data is processed.

Table 13. Total Power consumption [mW] for LP model in case of full memory

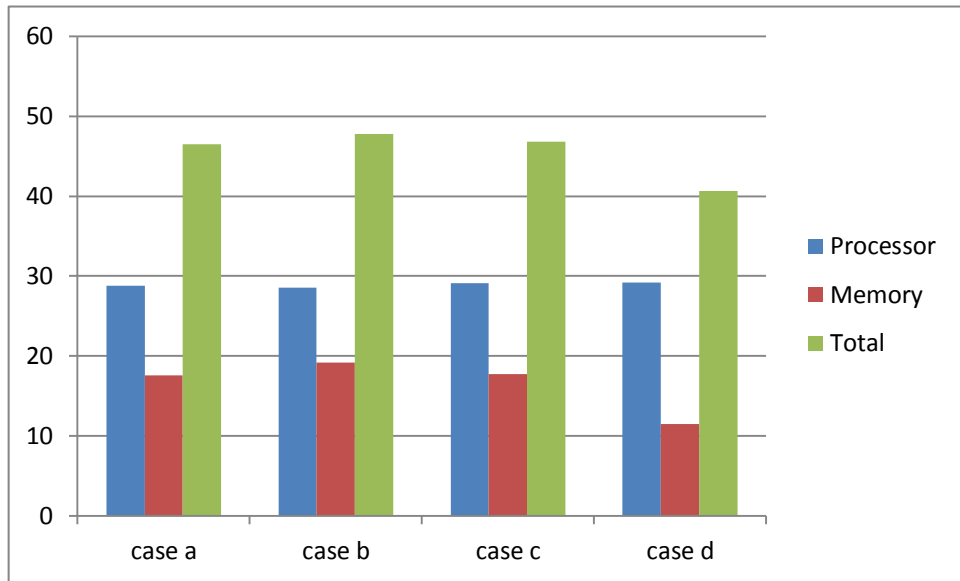
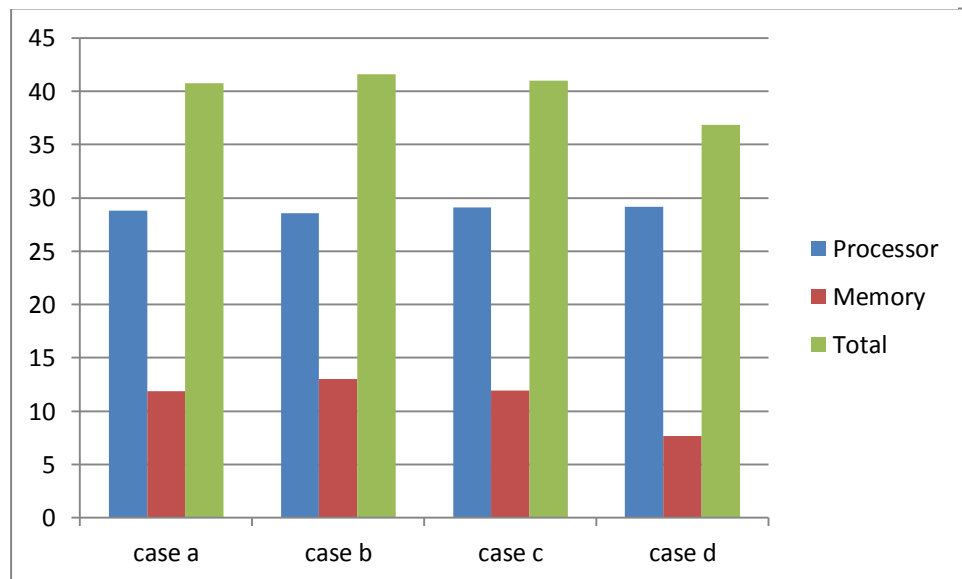


Table 14. Total Power consumption [mW] for LP model in case of half memory



By making comparison between the previous tables, it can be realized that the solution consumes more power in the case of full memory usage rather than the half memory. This conclusion clarifies the significance of the memory configuration on the power consumption.

5.4. Energy per Bit

Although in the beginning it was mentioned that the power consumption is better to be used for analysis, since the Tensilica itself claims that the power conversions are not very reliable, in the following the energy analysis results are also revealed.

The energy analysis is made for one $3.6\mu\text{s}$ time frame; the results include both leakage and dynamic portions of the energy. As the memory configuration does not have effect on the results, the memory capacity of 64K is assumed. Table 15 and Table 16 reveal the energy consumption for all the transmission scenarios blocks which are profiled in LP and PM configurations, respectively.

Table 15. Energy consumption [pJ] for each block in all transmission scenarios, LP, 64K

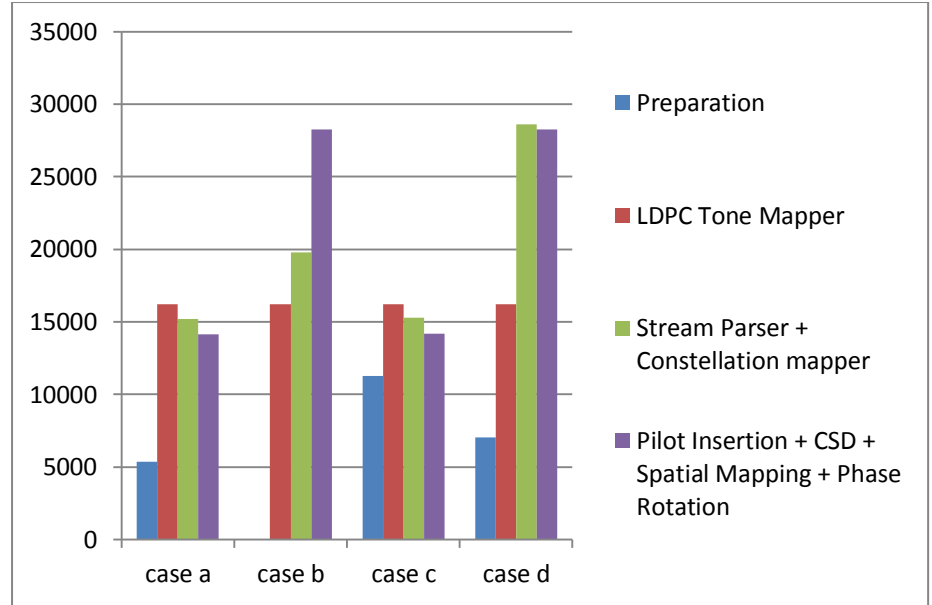
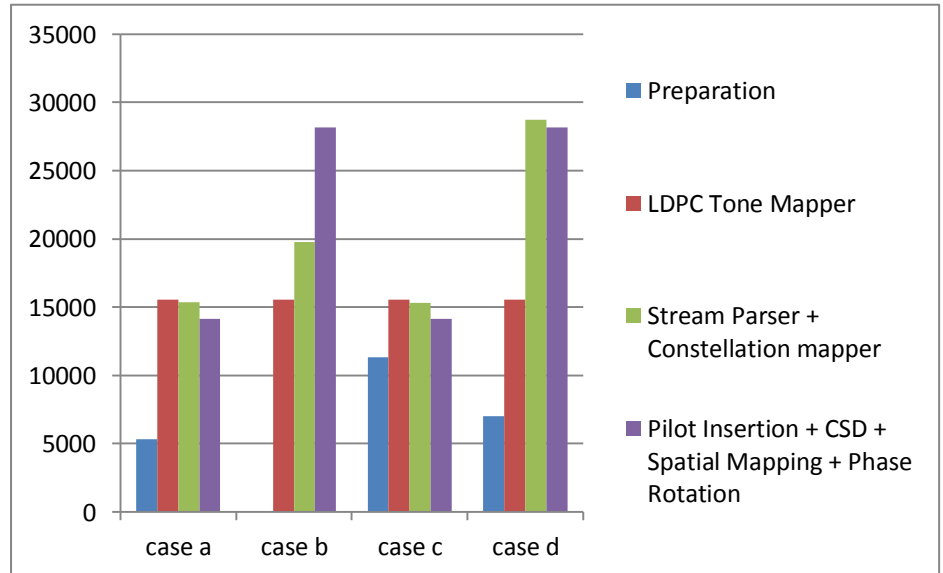


Table 16. Energy consumption [pJ] for each block in all transmission scenarios, PM, 64K



One of the useful assessment criteria to evaluate the solution is to find out the required energy for transferring one bit through the channel which is referred as energy per bit. It can be defined by dividing the total energy consumption by the total number of bits processed in the transmitter. The total number of bits for each transmission scenario is different and will be defined in the following. It shall be noticed that the evaluation is made for two processor configurations in the case of memory capacity of 64K.

In the first case, two spatial streams are processed which consist of 256×8 bits which mean $256 \times 8 \times 2$ bits are totally sort out. In this regard, the total energy consumption in case of LP and PM are divided by 4096 bits. In the second scenario, four spatial streams are processed so that 8192 bits are analyzed. In the third case, one spatial stream comes to the transmitter which means only 2048 bits should be taken into account. In the last case, two spatial streams are processed which is similar to the second case, and in total 4096 bits are handled. Table 17 shows the total energy consumption for all the transmission scenarios profiled in LP and PM configurations.

Table 17. Total energy [μ J] consumption for all the cases

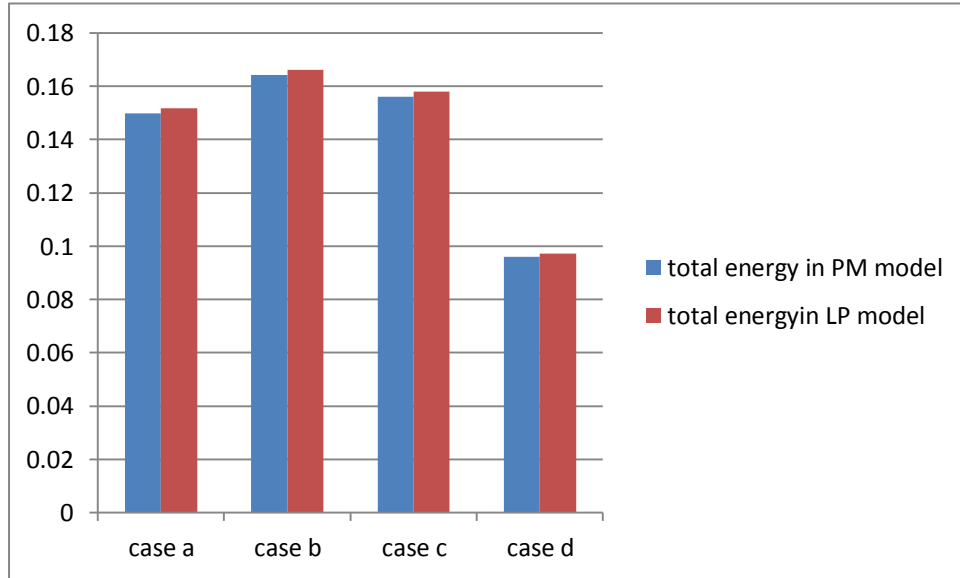


Table 18. Energy per bit [pJ] for all the cases

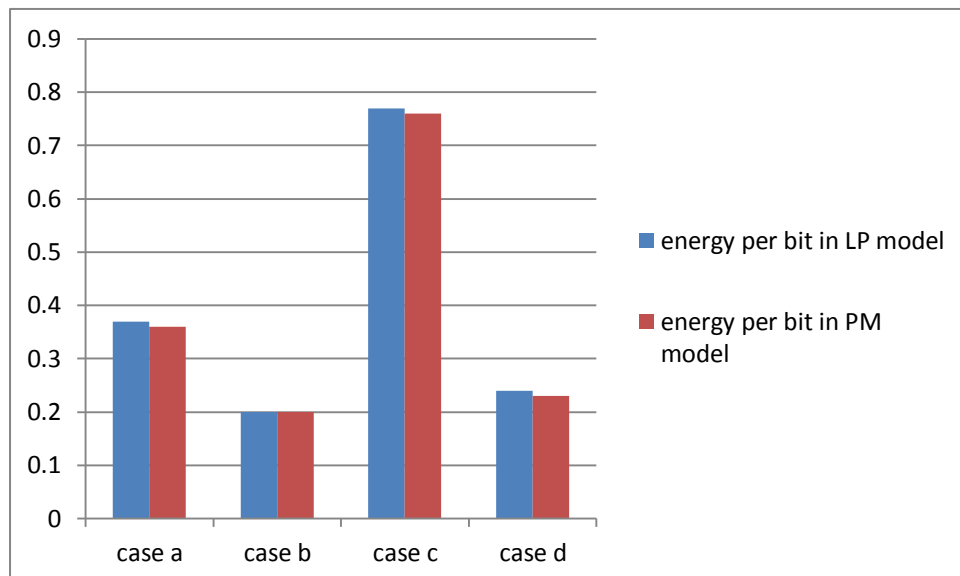


Table 18 shows the required energy for transmission of one bit for all the transmission scenarios. As it can be realized, the third case consumes more energy compared to the rest which is due to the fact that two spatial streams are processed to generate four space time streams by using STBC. Therefore, after STBC operations, four streams are analyzed. However, the second case requires lower energy as it is the simplest case in the implementation procedure due to the fact that it even does not need the preparation block in contrast with other scenarios. It is worth noticing that LP and PM configurations results do not considerably differ from each other in this term.

5.5. Memory Usage

One more evaluation parameter is the code size or memory usage. In this project as two memory categories are used including instruction and data, the evaluation is made for both of them.

It is worth noticing that among all the listed functions, only LDPC tone mapper and the last block including pilot insertion, spatial mapping, cyclic shift diversity and phase rotation are completely loop unrolled. As the loop unrolling increases the code size, the instruction memory usage for each transmission mode per each operation is presented in the following tables. Since there is no difference between PM and LP model from the memory usage point of view, only the results using the PM model are presented.

It should be noted that we have assumed that all incoming bits from the LDPC encoder are already stored in the local data memory. The data memory usage for each transmission mode is also reported at the same tables under ‘input buffer usage’ title, and it only depends on the transmission scenario.

Table 19 introduces the data and instruction memories usage for the all transmission mode. It should be noted that the first and second transmission cases does not have STBC process so that the reported values show only the instruction and data memories usage for preparation block.

As mentioned earlier, in order to speed up the processing, the numerical values of the last block including pilot insertion, cyclic shift diversity, spatial mapping and phase rotation were calculated and stored in a look-up table. This table occupies 128 and 800 bytes from the local data RAM#0 and RAM#1, respectively.

With reference to Table 19, it has been observed that LDPC tone takes more capacity among the functions. In addition, the amount of used data memory does not depend on the transmission scenario except for the input buffer usage.

As aforementioned, the utilized processor is an extended version of the Tensilica’s baseline DSP core and by exploiting additional extension instruction BBE32 will be configured. Thus, by profiling the total number of instructions (those which are started by BBE32 prefix) and their code size, useful information will be found out.

Table 19. Memory usage in bytes

Instruction Memory				
Block	Case a	Case b	Case c	Case d
Preparation + STBC	184	---	376	240
LDPC Tone Mapper	1808	1808	1808	1808
Stream Parser + Constellation Mapper	432	200	428	528
Pilot Insertion + CSD + Spatial Mapping + Phase Rotation	720	720	720	720
Total	3612	3664	3800	4232
Data memory				
Local Data RAM #0	4.8K			
Local Data RAM #1	5.128K			
Input Buffer	468	936	468	936
Total	10.396K	10.846K	10.396K	10.846K

Table 20 presents the total number of instructions and their size in the instruction memory for all the transmission scenarios.

Table 20. Instruction and code size

Parameter	Case a	Case b	Case c	Case d
Total number of Instructions	965	1102	1036	1255
Total size in data memory [bytes]	6977	7033	6980	7057

5.6. Analysis

As mentioned earlier, the developed software based implementation was profiled and analysed with the aid of the tools provided by the vendor. The analysis will be made on the results relating to number of clock cycles, power, energy, and memory usage.

The most important aspect linked to the clock cycle numbers is the real-time operation criteria. As previously mentioned, the duration of an OFDM symbol is $4\mu\text{s}$ for the header part and $3.6\mu\text{s}$ for the data part when short Guard Interval (GI) is used. Thus to achieve real-time operation in the transmitter, all the processing needed to create one OFDM symbol should not take more than $3.6\mu\text{s}$. Assuming a 500 MHz operating frequency, $3.6\mu\text{s}$ can accommodate 1800 clock cycles. Looking at the total number of clock cycles for each transmission scenario from Table 7 to Table 10, it can be concluded that the system operations can be computed in real-time in this implementation.

In term of power and energy consumption, according to the revealed results in power consumption and energy analysis sections, the total power consumption estimates are found adequately feasible to mobile terminal scale devices. By this means, the developed software solution is sufficiently applicable in the small size devices. The required

energy for one bit transmission was also revealed which showed the third case consumes more energy to transmit one bit.

From the code size and memory usage points of views, the solution is well organized and programmed as the memory usage tables show the results relating to different transmission scenarios.

5.7. Related Works

So far, a vast majority of the local area connectivity device implementations, in particular IEEE802.11ac related, are fixed-function solutions. As of today, some implementations have been done based on SDR, but most of the SDR platforms utilize a mix of software and hardware [53]. In the following, some of the recent and relevant works are reviewed.

In the work by Yoshizawa and Miyanaga [9], a VLSI implementation of a 4x4 MIMO Orthogonal Frequency Division Multiplexing (OFDM) transceiver with 80MHz transmission bandwidth is described, and tailored to a single transmission scenario of this thesis. According to the authors, they have only implemented one of the possible transmission scenarios, and the reported power consumption estimates are not feasible.

Although, some contributions have been also made towards the software defined radio concept, they are mainly focused on the MAC layer processing. In [10], Samadi et al. have addressed the design and implementation of the IEEE802.11 MAC layer processing using general-purpose DSP and additional accelerator systems.

In [54], IEEE802.11p transceiver architecture with SDR technology is proposed for the PHY layer processing in the Intelligent Transportation Systems (ITS). The power estimations are shown that the proposed architecture is not power efficient compared to this thesis. Similar work has been done in [55] by Knopp et al. which shows a better performance in term of time consumption and promises a real-time processing for specific operation schemes.

In [56], Eberli et al. have applied an Application Specific Instruction-Set Processor (ASIP) solution in the IEEE802.11a baseband receiver implementation. With the dedicated solution, they have been successful to achieve a real-time operation for data rate up to 54Mbps at the frequency clock of 160MHz which is surprisingly efficient in terms of time, cost and size.

Ramdurai et al. have described a software implementation of the IEEE802.11a receiver's challenging blocks like demapper, deinterleaver and depuncture [57]. They have also used a table lookup based method to merge these three functions for optimization purposes.

In [58], Agullo et al. have proposed and evaluated a software defined radio implementation of IEEE802.11 MAC with emphasis on cross-layer communications and networking. However, as it can be seen also in [11]-[14], only selected parts of PHY or MAC layer are typically targeted while other processing still relies on dedicated hardware.

In [59], Iacono et al. have implemented the IEEE802.11a/p receiver based on the SDR technology. Their main focus is also on the PHY specifications, but the data rate they have targeted is much lower than our case. Furthermore, the used modulation and coding schemes also differ which lead to different results. However, the comparison between the results shows that this project is dominant in terms of clock cycles and power consumption.

6. CONCLUSION

In this thesis, the feasibility of the software implementation of the IEEE802.11ac transmitter frequency domain baseband processing is studied. Our main focus was on the PHY layer implementation in four different multiantenna operation points which include 2x2 and 4x4 MIMO antenna configurations to achieve a data rate beyond 1Gbps. The employment of the higher number of spatial streams up to 4 streams, higher modulation order like 256-QAM scheme and wider bandwidth of 80MHz resulted in massive amount of data processing which can be carried out by the utilized DSP, ConnX BEE332.

The analysis of the performance numbers clearly shows that the developed software based implementation on a DSP core can achieve real-time operation for the transmitter baseband processing assuming 500 MHz clock frequency. Furthermore the implementation resulted in realistic power consumption and memory usage, despite of massive amount of data processing yielding beyond 1Gbps transmission bit rate in the most ambitious transmission scenario. In terms of power, as the power consumption estimates, in Chapter 5, showed the maximum value of 40mW; therefore, the proposed software implementation is found feasible to the mobile terminal scale devices.

Regarding the programmable SDR application in the baseband processing, it can be stated that the vector processors are well promising cores for scalable, flexible and adaptable parallel processing a huge amount of data. Consequently, in order to deal with newer wireless standards and multi operational standards devices, exploiting the vector processor is probably an appropriate choice to achieve low power consumption and cost to compete with other vendors. However, flexibility, compatibility, and adaptability can be solved with programmability, performance calls for certain processors. The performance can be increased by customizing the processor according to the needs of the application. If the application has inherent data parallelism, then vector processing or SIMD extensions can be used which are capable to provide energy-efficiency compared to general-purpose processor without customizations.

It is worth noticing that the software based implementation for the transmitter only includes the frequency domain PHY functions, in other words it does not provide the MAC layer functions and non-frequency domain functions such as IFFT. However, in order to provide a competitive implementation in the terms of power and area, both hardware and software designs need to be defined and assessed. In addition, the accuracy of the power and energy measurements is not certain and determined which lead to error in the results and evaluation. In order to measure the power, the platform must be implemented on the chip which is not done in this research. In the real-time evaluation,

we have not taken into account the time needed to receive all the data in the local memories. In fact, it has actually been assumed that all the data are already stored in the local data memories; hence the required time for data transfer to the local memory has not been considered.

In this thesis, we have also found that the customized VLIW processors with the vector processing capabilities provide highly improved flexibility, much faster time-to-market and more possibilities to bringing in new transmission features and enhancement. Meanwhile, the compatibility and adaptability problems in the conventional fixed-function modems can be conquered. As a result, by the rapid pace of wireless communications systems growth, we can be hopeful that the software based implementation can be upgraded. Thus, the entire system does not need to be replaced.

The future work will focus on implementing the corresponding receiver chain PHY processing which includes computationally more intensive processing such as channel state estimation and detection.

REFERENCES

- [1] D. Tse, P. Viswanath, Fundamental of Wireless Communications, Cambridge University Press, 2005.
- [2] L. Cinquino, A., R. Shayan, Y., A Real-Time Software Implementation of an OFDM Modem Suitable for Software Defined Radio, IEEE, 2004.
- [3] IEEE Standard for Information Technology–Telecommunications and Information Exchange between Systems and Local and Metropolitan Area Networks–Specific Requirements. Part 11: Wireless LAN Medium Access Control (MAC) and Physical Layer (PHY) Specifications, IEEE Std 802.11TM, 2012.
- [4] Quatenna Communications, An Introduction to IEEE802.11ac, Sigurd Schelstraete, September 2013.
- [5] R. Berger, C., Arbatov, V., Voronenko, Y., Franchetti, F., Puschel M., Real-Time Software Implementation of an IEEE802.11a Baseband receiver on Intel Multicore, ICAPP, 2011.
- [6] Wolf, W., Building the Software Radio, Computer, Vol. 38, No. 3, March 2005.
- [7] Koch, P., Prasad, R., The Universal Handset, IEEE Spectrum, Vol. 46, No. 4, April 2009.
- [8] V. Berkel, K., Heinle, F., P. E. Meuwissen, P., Moerman, K., Wiess, M., Vector Processing as an Enabler for Software Defined Radio in Handheld Devices, EURASIP Journal on Applied Signal Processing, 2005.
- [9] S. Yoshizawa and Y. Miyanaga, VLSI Implementation of a 4×4 MIMO-OFDM transceiver with an 80-MHz channel bandwidth, in Proc. ISCAS, Taipei, Taiwan, 24-27 May 2009, pp. 1743-1746.
- [10] S. Samadi, A. Golomohammadi, A. Jannesari, M.R. Movahedi, B. Khalaj, and S. Ghammanghami, A Novel Implementation of the IEEE802.11 Medium Access Control, in Proc. Int. Symp. Intelligent Signal Process. Commun., Yonago, Japan, 12-15 Dec. 2006, pp.489-492.
- [11] K. Rounioja, and K. Puusaari, Implementation of an HSDPA Receiver with a Customized Vector Processor, in Proc. Int. Symp. System-on-Chip, Tampere, Finland, 13-16 Nov. 2006, pp. 1-4.

- [12] W. Xu, M. Richter, M. Sauermann, F. Capar, and C. Grassmann, Efficient baseband implementation on an SDR platform, in Proc. Int. Conf. ITS Telecommunications, St. Petersburg, Russia, 23-25 Aug. 2011, pp.794-799.
- [13] J. Janhunen, T. Pitkänen, M. Juntti, and O. Silvén, Energy-efficient programmable processor implementation of LTE compliant MIMO-OFDM detector,” in Proc. ICASSP, Kyoto, Japan, 25-30 March 2012, pp. 3276 – 3279.
- [14] S. Eberli, A. Burg, and W. Fichtner, Implementation of a 2×2 MIMO-OFDM Receiver on an application specific processor, Microelectronics Journal, vol. 40, No. 11, pp. 1642-1649, November 2009.
- [15] IEEE global history network, Wireless LAN 802.11 Wi-Fi.
- [16] IEEE Standard Association [WWW]. [Accessed on 20.11.2013]. Available at: [<http://standards.ieee.org/about/ieeesa.html>]
- [17] Agilent Technologies, IEEE802.11Wireless LAN PHY Layer (RF) Operation and Measurement, USA, April 2002.
- [18] IEEE Standard for Information Technology–Telecommunications and Information Exchange between Systems and Local and Metropolitan Area Networks–Specific Requirements. Part 11: Wireless LAN Medium Access Control (MAC) and Physical Layer (PHY) Specifications, IEEE Std 802.11TM, 2013.
- [19] IEEE 802.11 WG, part 11a/11b/11g, Wireless LAN Medium Access Control (MAC) and Physical Layer (PHY) specifications, Standard Specification, IEEE,1999.
- [20] Eldad Perahia and Intel Corporation, IEEE802.11n Development: History, process, and Technology, July 2008, IEEE communications magazine.
- [21] Mamshaei, M. H., Cantieni, G. R., Barakat, C., Turletti, T., Performance Analysis of the IEEE802.11 MAC and PHY Layer Protocol, IEEE, June 2005.
- [22] Valadas, R.T., Tavares, A.R., Duarte, A.M.deO., Moreira, A.C., Lomba, C.T., The infrared physical layer of the IEEE 802.11 standard for wireless local area networks, Communications Magazine, IEEE , vol.36, no.12, pp.107-112, Dec 1998.
- [23] Pahlavan, K., H. Probert, T., E. Chase, M., Trends in Local Wireless Networks, IEEE Communications magazine, March 1995.

- [24] Aftab Ahmad, Data Communication principles: for fixed and wireless networks, 2003, Kluwer Academic Publisher.
- [25] Roshan, P., Leary, J., IEEE802.11 Wireless LAN Fundamentals, Indianapolis 2003, Cisco Press.
- [26] IEEE802.11b Wireless LANs; Wireless Freedom at Ethernet Speeds, Technical Paper, 3COM Corporation.
- [27] Perahia, E., Stacey, R., Next Generation Wireless LANs Throughput, Robustness, and Reliability in 802.11n, Cambridge University Press, 2008, Chapter 7.
- [28] Eldad Perahia, Robert Stacy, Next Generation Wireless LANs, Cambridge, 2nd edition, 2013.
- [29] Mohinder Jankiraman, Space-Time Codes and MIMO Systems, 2004, ARTECH House.
- [30] IEEE 802.11 WG. International standard for information technology – local and metropolitan area networks, part 11: wireless LAN MAC and PHY specifications, 1999.
- [31] Sylvester, A. U., Prince, A. O., Edward, O. E., Carrier Sensing Mechanisms: The Impact on Throughput Performance of IEEE 802.11WLANs, Scholar, Vol. 1, No. 1, March 2012.
- [32] Zheng Y., Lu k., Wu D., Performance analysis of IEEE 802.11 DCF in imperfect channels, ACM conference 2002.
- [33] P. Crow, B., Widjaja, I., Geun Kim, J., T. Sakai, P., IEEE802.11 Wireless Local Area Networks, IEEE Communications Magazine, Spetember 1997.
- [34] IEEE Standard 802.11-2007, Wireless LAN Medium Access Control (MAC) and Physical Layer (PHY) Specifications, June 2007.
- [35] Sikdar, B., Delay analysis of IEEE 802.11 PCF MAC based wireless networks, Global Telecommunications Conference, 2005. GLOBECOM '05. IEEE , vol.1, 28 Nov.-2 Dec. 2005.
- [36] Prasad, R., J. Velez, F., OFDM WI-MAX Physical Layer, Springer, 2010.
- [37] Qualcomm, IEEE802.11ac The next evolution of Wi-Fi standards, May 2012.

- [38] Roche, G., Glazunov, A. A., Allen, B., LTE-Advanced and Next Generation Wireless Networks: Channel modeling and propagation, Wiley, 2013.
- [39] Aruba White Paper, 802.11ac In-Depth,.
- [40] Tensilica Inc., ConnX BBE32 DSP user guide, USA, 2012.
- [41] Fosdick, D., R. Jessup, L., J. C. Shauble, E., Domik, G., An Introduction to High Performance Scientific ComputingThe Massachusetts Institute of Technology, 1996.
- [42] Asanovic, K., Vector Processors, Elsevier Science, 2003.
- [43] Flynn, M. J., Computer Architecture: Pipelined and Parallel Processor Design, Jones and Bartlett Publisher, 1995.
- [44] L. Null, J. Lobur, Computer Organization and Architecture, Jones and Bartlett Publisher, 2006.
- [45] Jadhav, S. S., Advanced Computer Architecture and Computing, Technical Publication Pune, 2009.
- [46] J., Dongarra, J., Hernandez, V., Vector and Parallel processing, VECPAR'98., Palma, Springer, 1998.
- [47] Censor, N., Parallel Optimization: Theory, Algorithm, and Application., 1997, Oxford.
- [48] NVIDIA SDR Technology, The modern innovation inside NVIDIA i500 and Tegra 4i, 2013.
- [49] Saksena, M., Selic, B., Real-Time Software Design- State of the Art and Future Challenges, IEEE Canadian Review, Summer 1999.
- [50] Tensilica Inc., ConnX BBE32 DSP Core for Baseband Processing, Configurable, Extensible and Scalable, USA, March 2013.
- [51] Tensilica Inc., ConnX BBE32 DSP Core for Baseband Processing, USA, 2013.
- [52] Draft Standard for Information Technology–Telecommunications and Information Exchange between Systems and Local and Metropolitan Area Networks–Specific Requirements. Part 11: Wireless LAN Medium Access Control (MAC) and Physical Layer (PHY) Specifications. Amendment 4: Enhancement for Very High

Throughput for Operation in Bands below 6GHz. IEEE P802.11acTM: D5.0, New York, January 2013.

- [53] Anjum, O., Ahonen, T., Garzia, F., Nurmi, J., Brunelli, C., Berg, H., State of the art baseband DSP platforms for softwaredefined radio: a survey, *EURASIP Journal on Wireless Communications and Networking*, 2011, 5.
- [54] Chen, Y.-H., A novel multicore SDR architecture for smart vehicle systems, *Proc. of the 12th Int. Conf. on Intelligent Transport Systems Telecommunications (ITST)*, November, 2012.
- [55] Schmidt-Knorreck, C., Knorreck, D., Knopp, R., IEEE 802.11p receiver design for software defined radio platforms, *DSD 2012, 15th Euromicro Conference on Digital System Design*, 5 – 8 September, 2012, Cesme, Izmir, Turkey.
- [56] Eberli, S., Burg, A., Bösch, T., & Fichtner, W., An IEEE 802.11a baseband receiver implementation on an Application Specific Processor, *Proceedings of IEEE Midwest Symposium on circuit & Systems*, Montreal, Quebec, Canada, pp. 1324 – 1327, Aug 2007.
- [57] Ramadurai, V., Jinturkar, S., Agarwal, S., Moudgill, M., Glossner, J., Software Implementation of 802.11a blocks on Sandblaster DSP, *Proceedings of Software Defined Radio Technical Forum*, Orlando Florida, November, 2006.
- [58] J.R. Gutierrez-Agullo, B. Coll-Perales, J. Gozalvez, An IEEE 802.11 MAC Software Defined Radio implementation for experimental wireless communications and networking research, in *Proc. IFIP Wireless Days*, Venice, Italy, 20-22 Oct. 2010, pp.1-5.
- [59] Lo Iacono, D., Cupaiuolo, T., Power Efficient SDR Implementation of IEEE802.11a/p Physical Layer, Springer, 2013.

APPENDIX 1: CLOCK CYCLE RESULTS

Clock cycle results for case a

Block Name	LP	PM
Preparation block	53	53
LDPC Tone Mapper	165	159
Stream parser + Constellation Mapper	150	153
Pilot Insertion + CSD + Phase Rotation + Spatial Mapping	130	130
Total number of clock cycles	507	495

Clock cycle results for case b

Block Name	LP	PM
Preparation	0	0
LDPC tone Mapper	165	159
Stream Parser + Constellation Mapper	197	197
Pilot Insertion + CSD + Spatial Mapping + Phase Rotation	260	210
Total number of Clock Cycles	622	616

Clock cycle results for case c

Block Name	LP	PM
Preparation + STBC	111	111
Stream Parser + Constellation Mapper	153	153
LDPC Tone Mapper	165	159
Pilot Insertion + CSD + Spatial Mapping + Phase Rotation	134	136
Total number of Clock Cycles	563	559

Clock cycle results for case d

Block Name	LP	PM
Preparation + STBC	68	68
Stream Parser + Constellation Mapper	300	300
LDPC Tone Mapper	165	159
Pilot Insertion + CSD + Spatial Mapping + Phase Rotation	268	256
Total number of Clock Cycles	801	783